Figure 5. Melanoma tumorigenesis is significantly suppressed in POSTN gene knockout mice. Macroscopic feature of the Rag2 KO and POSTN/Rag2 KO mice on the day 56 after human melanoma cell implantation (A). There was decreased expression of Ki-67, αSMA, and collagen in the tumors of POSTN/Rag2 KO mice. Dermal myofibroblast is positive for αSMA staining and collagen tissue becomes red by E-V (Elastica van Gieson) staining. Bar indicates 250 μm (B). There was a significant decrease in the number of Ki-67-positive cells in POSTN/Rag2 KO mice (C). There was significant suppression of melanoma tumorigenesis in POSTN gene knockout mice (D). *, **, and *** indicate P-value <0.05, <0.01, <0.001, respectively.

novel mechanism(s) of action, which are not associated with such life-threatening adverse events. We believe that POSTN is important for the growth of melanoma, because the implanted melanoma cell grew more slowly in POSTN-depleted mice compared with matched control mice. A therapeutic approach targeting POSTN and its related signaling may lead to a safer treatment for malignant melanoma, and one that is less likely to be thwarted by resistance of the cancer cells.

In this experimental setting, there was no significant improvement in the overall survival in the POSTN-depleted mice even though the tumor growth was attenuated in KO mice compared with control mice on an immune-deficient background. There is no doubt that the survival is strongly dependent on the metastasis of the inoculated tumor cells, but we did not observe any metastasis in either the KO or wild-type mice, which likely contributed to the lack of a difference in the overall survival between the groups.

In conclusion, in human melanoma tissue, NHDFs interacted with melanoma cells to induce POSTN, which directly promoted melanoma cell proliferation by activating integrin/p44/42MAPK signals and indirectly instituted a fibrotic microenvironment in the tumor, thus resulting in

a progression of the melanoma. As a result, the suppression of POSTN represents a novel therapeutic target for cutaneous malignant melanoma.

Methods

Cells and tissue samples

Human melanoma cell lines (MeWo, G-361, and VMRC-MELG) were obtained from the Japanese Collection of Research Bioresources (JCRB, Osaka, Japan), and NHDFs were obtained from TaKaRa Bio (Shiga, Japan). 293, 231, and A549 were represented by HEK293, MDA-MB-231, and A549 cancer cell lines loaded as positive controls, respectively (JCRB). All melanoma and normal tissue samples were obtained from patients at Osaka University Hospital (Department of Dermatology, Osaka, Japan). All clinical samples were collected after approval was obtained from the local ethics committee, and informed consent was obtained from each patient for use of the samples. Details of cell culture are described in Data S1.

Mice

Twelve-week-old Rag2-deficient $(Rag2^{-/-}$, C57BL/6 background) and periostin-deficient $(Postn^{-/-}$, C57BL/6 background) mice were used for the studies (Shimazaki et al., 2010). Experiments were undertaken following the guidelines for the care and use of experimental animals as required by the Japanese Association for Laboratory Animals Science (1987).

Sample preparation and iTRAQ labeling

Proteins were extracted from the frozen tumor and normal skin tissue samples. Details are described in Data S1.

Extracted proteins were purified using a 2D clean-up kit (GE Healthcare, Buckinghamshire, UK). Subsequently, 100 µg of each protein was dissolved, reduced, alkylated, and digested with trypsin, according to the manufacturer's protocol (Applied Biosystems, Foster City, CA, USA). The samples were labeled with iTRAQ reagent: reagent 114 for melanoma in situ, reagent 115 for normal skin lesions of melanoma in situ, reagent 116 for invasive melanoma, and reagent 117 for normal skin lesions of invasive melanoma. The labeled peptide samples were mixed and fractionated as described previously (Serada et al., 2010).

Mass spectrometric analysis and iTRAQ data analysis

NanoLC-MS/MS analyses and iTRAQ data analysis were performed as described in Data S1.

Western blot analysis

Cell lysates and supernatant fluids were used for the Western blot analyses. Details were described in Data S1.

Immunohistochemistry

Patient with paraffin-embedded melanoma tissue sections and in vivo mice melanoma tissue sections were stained with hematoxylin and eosin (H&E). For the immunohistochemical analysis, primary antibodies were used at the following dilutions: the human and mouse anti-POSTN (1:3000; Abcam, Tokyo, Japan), mouse anti-Ki-67 (1:500; Novocastra Laboratories Ltd, Newcastle, UK), and mouse anti-α-smooth muscle actin (α-SMA; 1:3000 dilution; Sigma-Aldrich, St. Louis, MO, USA). Details are described in Data S1.

Reverse transcription polymerase chain reaction (RT-PCR) analysis

To confirm the altered expression of POSTN in melanoma cells and NHDFs, melanoma cells (MeWo, G-361, and VMRC-MELG), NHDFs, and the cocultured cell samples were subjected to RT-PCR. β-actin was used as a housekeeping gene to evaluate and compare the quality of different cDNA samples. The primer sequences and the expected sizes of PCR products were as follows:

periostin, forward, 5′-TTGAGACGCTGGAAGGAAAT-3′
reverse, 5′-AGATCCGTGAAGGTGGTTTG-3′ (199 bp);
β-actin, forward, 5′-AGCCTCGCCTTTGCCGA-3′
reverse, 5′-CTGGTGCCTGGGGCG-3′(174 bp);

Details of total RNA extraction, quantitect reverse transcription, and RT-PCR are described in Data S1.

Quantitative reverse transcription polymerase chain reaction (qT-PCR) analysis

Normal human dermal fibroblasts were cocultured with CFSE-labeled MeWo and G-361 cells for 24 h. Thereafter, we sorted these cells into NHDF, MeWo, and G-361 cells using a FACS system. Next, the total RNA was isolated from the sorted NHDF, MeWo, and G-361 cells, and the products were reverse-transcribed into cDNA. The expression of TGFβ1, TGFβ3, IL-4, IL-13, BMP2, and PDGF-bb was measured using the Power SYBR Green PCR Master Mix (Applied Biosystems, Tokyo, Japan) according to the manufacturer's protocol. Glyceraldehyde-3-phosphate dehydrogenase (GAPDH) was used to normalize the mRNA, as GAPDH was not affected by the treatment. The primer sequences used were as follows:

TGFβ1, forward, 5′-TCGCCAGAGTGGTTATCTTTTG-3′

reverse, 5′-AGGAGCAGTGGGCGCTAAG-3′;
TGFβ3, forward, 5′-GCCCTTGCCCATACCTCCGC-3′
reverse, 5′-CGCAGCAAGGCGAGGCAGAT-3′;
GAPDH, forward, 5′-GGAGTCAACGGATTTGGTCGTA-3′
reverse, 5′-GCAACAATATCCACTTTACCAGAGTTAA-3′;
IL-4, forward, 5′-ACATTGTCACTGCAAATCGACACC-3′
reverse, 5′-TGTCTGTTACGGTCAACTCGGTGC-3′;
IL-13, forward, 5′-GCAATGGCAGCATGGTATGG-3′
reverse, 5′-AAGGAATTTTACCCCTCCCTAACC-3′;
BMP2, forward, 5′-ACTCGAAATTCCCCGTGACC-3′
reverse, 5′-CCACTTCCACCACGAATCCA-3′;
PDGF-bb, forward, 5′-CAGCGCCCATTTTTCATTCC-3′
reverse, 5′-GTTTTCTCTTTGCAGCGAGGC-3′.

Construction of a NHDF-derived POSTN expression vector

To construct a NHDF-derived POSTN expression vector, the cDNA of human POSTN derived from NHDFs cocultured with melanoma cells was amplified. The amplified cDNA was then inserted into the pcDNA3.1/V5-His-TOPO vector (Invitrogen, Carlsbad, CA, USA) and designated pcDNA3.1-POSTN.

Generation of NHDF-derived POSTN stable transfectant melanoma cells

To generate NHDF-derived POSTN stable transfectant cells (POSTN–MeWo), the MeWo cell line was transfected with pcDNA3.1-POSTN using Lipofectamine 2000 (Invitrogen) according to the manufacturer's instructions, after which the cells were selected with 500 µg/ml of Geneticin (GIBCO; Invitrogen). Stable clones were maintained in 250 µg/ml of Geneticin.

Proliferation assay

The proliferation of MeWo, G-361, VMRC-MELG, and POSTN–MeWo melanoma cells was examined using the Cell Counting Reagent SF (Nacalai Tesque, Kyoto, Japan) according to the manufacturer's recommendations, and then, absorbance was measured with a microplate reader (model 680; Bio-Rad, Tokyo, Japan) at test and reference wavelengths of 450 and 630 nm, respectively.

Kinase inhibition assays

The cells were incubated for 2 h with kinase inhibitors (Cell Signaling Technology, Beverly, MA, USA): LY294002 (10 µM) as an Akt inhibitor and PD98095 (10 µM) as a MAPK inhibitor. Cells were then stimulated with 100 ng/ml of recombinant POSTN in the same media. After stimulation, the MTT proliferation assay was performed.

Statistical analyses

The results are presented as the means + SD. The analyses were carried out using the two-sided, unpaired Student's t test or the two-sided Welch test. Multiple comparisons between groups were made by Fisher's or Dunnett's methods. We considered values to be significant when $P < 0.05$.

Acknowledgements

637

Disclosure statement

All authors declare no financial support or relationship that may pose conflict of interest.

References

Asano Y, I.H., Yamane K, J.M., Mimura, Y., and Tamaki, K. (2005). Increased expression of integrin alpha(v)beta3 contributes to the establishment of autocrine TGF-beta signaling in scleroderma fibroblasts. J. Immunol. *175*, 7708–7718.

Atefi, M., von Euw, E., Attar, N. et al. (2011). Reversing melanoma cross-resistance to BRAF and MEK inhibitors by co-targeting the AKT/mTOR pathway. PLoS ONE *6*, e28973.

Bao, S., Ouyang, G., Bai, X. et al. (2004). Periostin potently promotes metastatic growth of colon cancer by augmenting cell survival via the Akt/PKB pathway. Cancer Cell *5*, 329–339.

Baril, P., Gangeswaran, R., Mahon, P.C. et al. (2007). Periostin promotes invasiveness and resistance of pancreatic cancer cells to hypoxia-induced cell death: role of the beta4 integrin and the PI3k pathway. Oncogene *26*, 2082–2094.

Elliott, C.G., Wang, J., Guo, X. et al. (2012). Periostin modulates myofibroblast differentiation during full-thickness cutaneous wound repair. J. Cell Sci. *125*, 121–132.

Erkan, M., Kleeff, J., Gorbachevski, A. et al. (2007). Periostin creates a tumor-supportive microenvironment in the pancreas by sustaining fibrogenic stellate cell activity. Gastroenterology *132*, 1447–1464.

Flaherty, K.T., Puzanov, I., Kim, K.B. et al. (2010). Inhibition of mutated, activated BRAF in metastatic melanoma. N. Engl. J. Med. *363*, 809–819.

Gillan, L., Matei, D., Fishman, D.A., Gerbin, C.S., Karlan, B.Y., and Chang, D.D. (2002). Periostin secreted by epithelial ovarian carcinoma is a ligand for alpha(V)beta(3) and alpha(V)beta(5) integrins and promotes cell motility. Cancer Res. *62*, 5358–5364.

Guarino, M. (2010). Src signaling in cancer invasion. J. Cell. Physiol. *223*, 14–26.

Hanahan, D., and Weinberg, R.A. (2000). The hallmarks of cancer. Cell *100*, 57–70.

Horiuchi, K., Amizuka, N., Takeshita, S. et al. (1999). Identification and characterization of a novel protein, periostin, with restricted expression to periosteum and periodontal ligament and increased expression by transforming growth factor beta. J. Bone Miner. Res. *14*, 1239–1249.

Inai, K., Norris, R.A., Hoffman, S., Markwald, R.R., and Sugi, Y. (2008). BMP-2 induces cell migration and periostin expression during atrioventricular valvulogenesis. Dev. Biol. *315*, 383–396.

Kudo, Y., Ogawa, I., Kitajima, S. et al. (2006). Periostin promotes invasion and anchorage-independent growth in the metastatic process of head and neck cancer. Cancer Res. *66*, 6928–6935.

Li, J.S., Sun, G.W., Wei, X.Y., and Tang, W.H. (2002). Expression of periostin and its clinicopathological relevance in gastric cancer. World J. Gastroenterol. *13*, 5261–5266.

Li, G., Oparil, S., Sanders, J.M. et al. (2006). Phosphatidylinositol-3-kinase signaling mediates vascular smooth muscle cell expression of periostin in vivo and in vitro. Atherosclerosis *188*, 292–300.

Nyberg, P., Salo, T., and Kalluri, R. (2008). Tumor microenvironment and angiogenesis. Front Biosci. *13*, 6537–6553.

Ontsuka, K., Kotobuki, Y., Shiraishi, H. et al. (2012). Periostin, a matricellular protein, accelerates cutaneous wound repair by activating dermal fibroblasts. Exp. Dermatol. *21*, 331–336.

Ouyang, G., Liu, M., Ruan, K., Song, G., Mao, Y., and Bao, S. (2009). Upregulated expression of periostin by hypoxia in non-small-cell lung cancer cells promotes cell survival via the Akt/PKB pathway. Cancer Lett. *281*, 213–219.

Polyak, K., and Kalluri, R. (2010). The role of the microenvironment in mammary gland development and cancer. Cold Spring Harb. Perspect. Biol. *2*, a003244.

Puppin, C., Fabbro, D., Dima, M. et al. (2008). High periostin expression correlates with aggressiveness in papillary thyroid carcinomas. J. Endocrinol. *197*, 401–408.

Quaranta, V. (2002). Motility cues in the tumor microenvironment. Differentiation *70*, 590–598.

Riener, M.O., Fritzsche, F.R., Soll, C. et al. (2010). Expression of the extracellular matrix protein periostin in liver tumours and bile duct carcinomas. Histopathology *56*, 600–606.

Sasaki, H., Dai, M., Auclair, D. et al. (2001). Serum level of the periostin, a homologue of an insect cell adhesion molecule, as a prognostic marker in nonsmall cell lung carcinomas. Cancer *92*, 843–848.

Sasaki, H., Sato, Y., Kondo, S. et al. (2002). Expression of the periostin mRNA level in neuroblastoma. J. Pediatr. Surg. *37*, 1293–1297.

Sasaki, H., Yu, C.Y., Dai, M. et al. (2003). Elevated serum periostin levels in patients with bone metastases from breast but not lung cancer. Breast Cancer Res. Treat. *77*, 245–252.

Serada, S., Fujimoto, M., Ogata, A. et al. (2010). iTRAQ-based proteomic identification of leucine-rich alpha-2 glycoprotein as a novel inflammatory biomarker in autoimmune diseases. Ann. Rheum. Dis. *69*, 770–774.

Shao, R., Bao, S., Bai, X. et al. (2004). Acquired expression of periostin by human breast cancers promotes tumor angiogenesis through up-regulation of vascular endothelial growth factor receptor 2 expression. Mol. Cell. Biol. *24*, 3992–4003.

Shimazaki, M., Nakamura, K., Kii, I. et al. (2010). Periostin is essential for cardiac healing after acute myocardial infarction. J. Exp. Med. *205*, 295–303.

Soltermann, A., Ossola, R., Kilgus-Hawelski, S. et al. (2008a). N-glycoprotein profiling of lung adenocarcinoma pleural effusions by shotgun proteomics. Cancer *114*, 124–133.

Soltermann, A., Tischler, V., Arbogast, S. et al. (2008b). Prognostic significance of epithelial-mesenchymal and mesenchymal-epithelial transition protein expression in non-small cell lung cancer. Clin. Cancer Res. *14*, 7430–7437.

Takayama, G., Arima, K., Kanaji, T. et al. (2006). Periostin: a novel component of subepithelial fibrosis of bronchial asthma downstream of IL-4 and IL-13 signals. J. Allergy Clin. Immunol. *118*, 98–104.

Takeshita, S., Kikuno, R., Tezuka, K., and Amann, E. (1993). Osteoblast-specific factor 2: cloning of a putative bone adhesion protein with homology with the insect protein fasciclin I. Biochem. J. *294*(Pt 1), 271–278.

Tilman, G., Mattiussi, M., Brasseur, F., van Baren, N., and Decottignies, A. (2007). Human periostin gene expression in normal tissues, tumors and melanoma: evidences for periostin production by both stromal and melanoma cells. Mol. Cancer. *6*, 80.

Tischler, V., Fritzsche, F.R., Wild, P.J. et al. (2010). Periostin is up-regulated in high grade and high stage prostate cancer. BMC Cancer *10*, 273.

Weber, J. (2008). Overcoming immunologic tolerance to melanoma: targeting CTLA-4 with ipilimumab (MDX-010). Oncologist *13*(Suppl 4), 16–25.

Yan, W., and Shao, R. (2006). Transduction of a mesenchyme-specific gene periostin into 293T cells induces cell invasive activity through epithelial-mesenchymal transformation. J. Biol. Chem. *281*, 19700–19708.

Yang, C., Zeisberg, M., Lively, J.C., Nyberg, P., Afdhal, N., and Kalluri, R. (2003). Integrin alpha1beta1 and alpha2beta1 are the key regulators of hepatocarcinoma cell invasion across the fibrotic matrix microenvironment. Cancer Res. *63*, 8312–8317.

Yang, L., Serada, S., Fujimoto, M. et al. (2012). Periostin facilitates skin sclerosis via PI3K/Akt dependent mechanism in a mouse model of scleroderma. PLoS ONE 7, e41994.

Zeisberg, M., Maeshima, Y., Mosterman, B., and Kalluri, R. (2002). Renal fibrosis. Extracellular matrix microenvironment regulates migratory behavior of activated tubular epithelial cells. Am. J. Pathol. *160*, 2001–2008.

Supporting information

Additional Supporting Information may be found in the online version of this article:

Table S1. List of all proteins identified by iTraq.
Data S1. Methods.

The translation elongation factor eEF2 is a novel tumor-associated antigen overexpressed in various types of cancers

YUSUKE OJI[1], NAOYA TATSUMI[1], MARI FUKUDA[2], SHIN-ICHI NAKATSUKA[12], SAYAKA AOYAGI[2], ERIKA HIRATA[2], ISAMU NANCHI[2], FUMIHIRO FUJIKI[3], HIROKO NAKAJIMA[3], YUMIKO YAMAMOTO[2], SYOHEI SHIBATA[2], MICHIYO NAKAMURA[2], KANA HASEGAWA[1], SAYAKA TAKAGI[2], IKUYO FUKUDA[2], TOMOKO HOSHIKAWA[2], YUI MURAKAMI[2], MASAHIDE MORI[13], MASAYOSHI INOUE[4], TETSUJI NAKA[5], TAKESHI TOMONAGA[15], YOSHIFUMI SHIMIZU[16], MASASHI NAKAGAWA[17], JUNICHI HASEGAWA[18], RIICHIRO NEZU[18], HIDENORI INOHARA[6], SHUICHI IZUMOTO[7], NORIO NONOMURA[8], TOSHIKI YOSHIMINE[7], MEINOSHIN OKUMURA[4], EIICHI MORII[9], HAJIME MAEDA[14], SUMIYUKI NISHIDA[10], NAOKI HOSEN[11], AKIHIRO TSUBOI[10], YOSHIHIRO OKA[5] and HARUO SUGIYAMA[2]

Departments of [1]Cancer Stem Cell Biology, [2]Functional Diagnostic Science, [3]Cancer Immunology, [4]Surgery, [5]Respiratory Medicine and Allergy, Rheumatic Diseases, [6]Otolaryngology and Sensory Organ Surgery, [7]Neurosurgery, [8]Urology, [9]Pathology, [10]Cancer Immunotherapy, and [11]Biomedical Informatics, Osaka University Graduate School of Medicine, Osaka; [12]Department of Pathology, Kansai Rosai Hospital, Hyogo; Departments of [13]Thoracic Oncology, and [14]General Thoracic Surgery, Toneyama National Hospital; [15]Laboratory of Proteome Research, National Institute of Biomedical Innovation, Osaka; [16]Department of Internal Medicine, Takarazuka City Hospital, Hyogo; [17]Department of Internal Medicine, Nissay Hospital; [18]Department of Surgery, Osaka Rosai Hospital, Osaka, Japan

Abstract. Recent studies have shown that cancer immunotherapy could be a promising therapeutic approach for the treatment of cancer. In the present study, to identify novel tumor-associated antigens (TAAs), the proteins expressed in a panel of cancer cells were serologically screened by immunoblot analysis and the eukaryotic elongation factor 2 (eEF2) was identified as an antigen that was recognized by IgG autoantibody in sera from a group of patients with head and neck squamous cell carcinoma (HNSCC) or colon cancer. Enzyme-linked immunosorbent assay showed that serum eEF2 IgG Ab levels were significantly higher in colorectal and gastric cancer patients compared to healthy individuals. Immunohistochemistry experiments showed that the eEF2 protein was overexpressed in the majority of lung, esophageal, pancreatic, breast and prostate cancers, HNSCC, glioblastoma multiforme and non-Hodgkin's lymphoma (NHL). Knockdown of eEF2 by short hairpin RNA (shRNA) significantly inhibited the growth in four eEF2-expressing cell lines, PC14 lung cancer, PCI6 pancreatic cancer, HT1080 fibrosarcoma and A172 glioblastoma cells, but not in eEF2-undetectable MCF7 cells. Furthermore, eEF2-derived 9-mer peptides, EF786 (eEF2 786-794 aa) and EF292 (eEF2 292-300 aa), elicited cytotoxic T lymphocyte (CTL) responses in peripheral blood mononuclear cells (PBMCs) from an HLA-A*24:02- and an HLA-A*02:01-positive healthy donor, respectively, in an HLA-A-restricted manner. These results indicated that the *eEF2* gene is overexpressed in the majority of several types of cancers and plays an oncogenic role in cancer cell growth. Moreover, the *eEF2* gene product is immunogenic and a promising target molecule of cancer immunotherapy for several types of cancers.

Introduction

Cancer immunotherapy consists of therapeutic approaches to elicit effective antitumor immunity through active or passive immunization. Recent studies have shown that cancer immunotherapy have potential to provide anticancer activity as a single agent or in combination with conventional surgery, radiation and chemotherapy as reviewed (1-4). These findings indicate that cancer immunotherapy should be a promising therapeutic option for the cancer treatment.

Strategies of cancer immunotherapy include antitumor monoclonal antibodies, cancer vaccines, adoptive transfer

of *ex vivo* activated T and natural killer cells, and administration of antibodies or recombinant proteins that either costimulate immune cells or block immune inhibitory pathways (5). Among these strategies, cancer vaccines are approaches to specifically activate host T cells against tumor antigens. The target antigens of cancer vaccine should be: i) highly immunogenic; ii) expressed in a significant proportion of cancer patients; iii) not expressed (or expressed in limited populations) in normal tissues; and iv) required for cancer cell growth and/or survival. Although large number of tumor-associated antigens (TAAs) have been identified using recently developed new technologies such as SEREX and protein microarrays (6,7), there are limited number of antigens that fit all of these criteria in current cancer vaccines.

High level protein biosynthesis is one of the characteristics of cancer cell metabolism (8). Translation is regulated at the initiation and elongation step and deregulated in cancer through a variety of mechanisms (9). Eukaryotic elongation factor 2 (*eEF2*) is a gene that plays an essential role in the polypeptide chain elongation step. Cells control translation levels at elongation step through regulation of eEF2 activity under multiple biological conditions such as cell cycle progression (10) and genotoxic stress (11,12), or in response to endogenous carbon monoxide that exerts antiproliferative effects (13). Previously, we showed that eEF2 was overexpressed in the majority of gastric and colorectal cancers and promoted progression of G_2/M of the cell cycle in association with activation of Akt and a G_2/M regulator, cdc2 proteins, resulting in the enhancement of *in vitro* and *in vivo* cancer cell growth (14). However, the role for eEF2 in the tumorigenesis remains largely unknown and it is undetermined whether eEF2 can be a target molecule of molecule-targeted cancer therapy.

In the present study, we identified eEF2 as an antigen eliciting humoral immune responses in a group of patients with HNSCC or colorectal cancer by immunoblot analysis and showed that eEF2 was overexpressed in the majority of various types of cancers such as lung, esophageal, pancreatic, breast and prostate cancers, HNSCC, glioblastoma multiforme and NHL. Knockdown of eEF2 by shRNA significantly inhibited growth of cancer cells. Furthermore, eEF2-derived 9-mer peptides, EF786 (eEF2 786-794 aa) and EF292 (eEF2 292-300 aa), elicited cytotoxic T lymphocyte (CTL) responses in PBMCs from an HLA-A*24:02- and an HLA-A*02:01-positive healthy donors, respectively, in an HLA-A-restricted manner.

Materials and methods

Cell lines. Lung cancer cell lines PC14 and LU99B, pancreatic cancer cell line PCI6, glioblastoma cell line A172, fibrosarcoma cell line HT1080, gastric cancer cell lines MKN28 and AZ-521, and breast cancer cell line MCF7 were cultured in Dulbecco's modified essential medium supplemented with 10% fetal bovine serum (FBS). Leukemia cell line K562, colon cancer cell line SW480, parent T2 and T2 cells with forced expression of either HLA-A24:02 (T2-2402) (15) or HLA-A02:01 (T2-0201) (16) were cultured in RPMI-1640 medium supplemented with 10% FBS. Leukemia cell line TF-1 was cultured in RPMI-1640 medium supplemented with 10% FBS containing 2 ng/ml human recombinant GM-CSF (Peprotech, Rocky Hill, NJ, USA).

Sera samples. Sera were obtained from 79 colorectal and 80 gastric cancer patients, 10 patients with head and neck squamous cell carcinoma (HNSCC) and 40 healthy individuals with informed consent at Osaka University Hospital and Osaka Rosai Hospital and stored at -80°C until use.

Tissue samples. Tumor tissues were obtained from 31 lung adenocarcinoma, 20 small-cell lung cancer, 15 esophageal squamous cell carcinoma, 21 HNSCC, 28 pancreatic cancer, 8 breast cancer, 16 glioblastoma, 4 prostate cancer and 50 NHL (40 diffuse large B-cell lymphoma and 10 folliclular lymphoma) patients. All samples were obtained with informed consent at Osaka University Hospital, Toneyama National Hospital, NHO Osaka Minami Medical Center, and Higashiosaka City General Hospital.

Western blot analysis. Proteins were separated by SDS-PAGE and transferred to Immobilon polyvinylidene difluoride membrane. After blocking of non-specific binding, the membranes were incubated with the first antibodies, followed by incubation with the corresponding secondary antibodies conjugated with alkaline phosphatase, and visualized using BCIP/NBT kit (Nacalai Tesque, Kyoto, Japan). Polyclonal anti-EF2 (Santa Cruz Biotechnology, Santa Cruz, CA, USA) and anti-GAPDH (Chemicon International, Temecula, CA, USA) were used as the first antibodies.

Density gradient isoelectric focusing. Density gradient isoelectric focusing was performed by the method reported previously (17) with minor modifications. In brief, K562 cells ($5x10^7$ cells) were lysed in 2 ml of 0.1% Triton X-100/PBS. After centrifugation, the supernatant was collected as cytoplasmic fraction. Proteins of the cytoplasmic fraction were precipitated with acetone and the pellet was solved in 1 ml of dH_2O containing 4% CHAPS and 7 M urea. Isoelectric focusing was carried out using an LKB column (NA-1720, Nihon-Eido Co., Tokyo, Japan) according to the manufacturer's instructions. On completion of the run, effluent fractions (3 ml each) were collected and twice dialyzed to 200 volume of de-ionized water for 18 h, and then the proteins were precipitated with acetone and stored at -80°C until use.

MALDI-TOF mass spectrometry. The bands on the silver stained gels were excised with surgical blazor. After dehydration with acetonitrile, the gel slice was dried with Speed Vac. The dried gels were digested with Trypsin (Promega, Madison, WI, USA) at 37°C for 24 h and the tryptic peptides were analyzed. All peptide mass fingerprinting (PMF) spectra were obtained by Matrix-assisted laser desorption/ionization time-of-flight (MALDI-TOF) mass spectrometry using an ultraflex spectrometer (Bruker Daltonics, Bremen, Germany). PMF data were then searched with MS-FIT software against NCBInr database.

Immunohistochemistry. Formalin-fixed tissue sections were cut from each paraffin-block. After dewaxing and rehydration, the sections were antigen retrieved using Pascal (Dako Cytometry, Glostrup, Denmark) and reacted with the first antibody at 4°C overnight and then reacted with Dako Envision kit/HRP (Dako Cytometry) at room temperature for 30 min.

After treatment with 3% H_2O_2 solution to reduce endogenous peroxidase activity, immunoreactive eEF2 protein was visualized using diaminobenzidine (DAB). The sections were then counterstained with hematoxylin. The intensity of stain in tumor cells was scored as positive (increased staining in carcinoma cells compared to that in normal cells) or negative (less or negative staining in carcinoma cells) by a pathologist. eEF2-H118 antibody (Santa Cruz Biotechnology) that recognized 741-858aa of eEF2 protein and Sigma-Aldrich #SAB4500695 antibody that recognized the N terminus of eEF2 protein were used as first antibodies. Non-immune rabbit immunoglobulin (Dako Cytometry) was used as negative control for non-specific staining.

Sequencing. The *eEF2* gene overexpressed in tumors was RT-PCR amplified and directly sequenced in both directions by the method previously described (14).

Transient expression of shRNA targeting eEF2. Two different shRNA vectors targeting eEF2 mRNA (shEF-1918 and shEF-2804 targeting 1918-1947 and 2804-2833 nt of eEF2 sequence, respectively) were prepared as described previously (14). shRNA targeting luciferase (shLuc) was used as a control. shRNA vectors were transiently expressed as described previously (14).

Enzyme-linked immunosorbent assay (ELISA). ELISA was established to measure serum eEF2 IgG Ab levels by a method previously reported (18) with modifications. ELISA 96-well plates were coated with recombinant GST-tagged eEF2 fragmented protein (Ref Seq NM_001961, 411-858 aa) (2 μg/well). Plates were blocked with TBS containing 0.05% Tween-20 and 1% gelatin. Sera were diluted at 1:100 in TBS containing 0.05% Tween-20 (0.05% TBST) and pre-absorbed by immobilized GST protein at 4°C overnight. Then, 100 μl of the diluted sera was added to each well for overnight incubation at 4°C. After washing, captured eEF2 IgG Ab was detected using ALP-conjugated goat anti-human IgG Ab (Santa Cruz Biotechnology) and BCIP/NBT kit. Then, absorbance at 550 nm was measured using a microplate reader. All sera were examined in duplicate. The titers of eEF2 IgG Ab were calculated by interpolation from the standard line which was constructed for each assay from the results of simultaneous measurements of serial dilutions of rabbit polyclonal eEF2 H-118 Ab using the corresponding second Ab (data not shown). eEF2 Ab titer that produces the absorbance at 550 nm equal to that produced by 1.0 μg/ml of eEF2 H-118 Ab in the ELISA system was defined as 1.0 EF2-reacting-unit (ERU).

Synthetic peptides. The primary amino acid sequence of human eEF2 was analyzed for consensus motifs for 9-mer peptides capable of binding to HLA-A*24:02 or 02:01 using ProPred-I computer algorithm (Table I). Then, the top 4 candidate peptides for HLA-A*02:01 and 24:02 each were synthesized at immunological grade (Sigma Genosys, Hokkaido, Japan). Synthesized peptide was solved in dH_2O (2 mg/ml) and stored at -20°C until use.

MHC stabilization assay. Binding of the synthetic peptides to HLA-A*24:02 or 02:01 molecules was evaluated by MHC stabilization assay using antigen processing mutant T2-2402 or T2-0201 cells as described previously (19). Expression of HLA-A24 or HLA-A02 molecules was measured with a FACSort flow cytometer (BD Biosciences, San Jose, CA, USA) and the mean fluorescence intensity (MFI) was recorded.

In vitro generation of eEF2 peptide-specific CD8⁺ T cells. PBMCs were obtained from an HLA-A*24:02-positive and an HLA-A*02:01-positive healthy donors by density gradient centrifugation. CD4⁺CD25⁺ Treg cells were depleted from PBMCs by using CD25 MicroBeads (Miltenyi Biotech, Auburn, CA, USA). For generation of autologous dendritic cells (DCs), CD14⁺ monocytes were isolated from the donor PBMCs using BD IMag CD14 isolation kit (BD Bioscience) and cultured in X-VIVO15 (Bio Whittaker, Walkersville, MD, USA) supplemented with 1% human AB serum (Nabi, Miami, FL, USA) containing IL-4 (1,000 U/ml) and GM-CSF (800 U/ml). After 24 h, IL-1β (10 ng/ml), IL-6 (1,000 U/ml), TNF-α (10 ng/ml), and PGE-2 (1 μg/ml) were added to the culture for DC maturation and the cells were cultured for 48 h. DCs were pulsed with EF2 peptide at the concentration of 10 μg/ml in X-VIVO15 supplemented with 1% human AB serum at 37°C for 2 h, irradiated at 30 Gy, and washed 3 times with RPMI-1640 medium. Then, Treg-depleted PBMCs (2x10⁶ cells) were stimulated by co-culture with the EF2 peptide-pulsed DCs at the DC: PBMC ratio of 1:10 in X-VIVO15 supplemented with 5% human AB serum. After 24 h of co-culture, IL-2 (20 U/ml) was added to the culture. The cultured cells were repeatedly stimulated with the EF2 peptide-pulsed, irradiated autologous PBMCs at 10-day intervals. After several times of re-stimulation, the cultured cells were maintained as the established T cell lines in X-VIVO15 supplemented with 5% human AB serum, IL-7 (10 IU/ml) and IL-15 (10 IU/ml) and used for cytotoxic assays.

⁵¹Cr release cytotoxicity assay. Effector cells were prepared from the established T cell lines using Human CD8 T Lymphocyte Enrichment Set-DM (BD Bioscience). Target cells (listed in Table III) were labeled with 100 μCi of ⁵¹Cr (Perkin-Elmer, Waltham, MA, USA) at 37°C for 1.5 h and the target cells (1x10⁴ cells) were added to wells containing varying numbers of effector cells in 96-well plates. After 4 h of incubation at 37°C, 100 μl of supernatants were collected from each well and measured for radioactivity. The percentage of specific lysis was calculated as follows: percentage of specific lysis = (cpm of experimental release - cpm of spontaneous release)x100/(cpm of maximal release - cpm of spontaneous release). Radioactivity of the supernatant of the target cells that were cultured without effector cells and the radioactivity of target cells that were completely lysed by the treatment with 1% Triton X-100 was used for spontaneous and maximal release, respectively. The characteristics of target cells in cytotoxicity assay are listed in Table III.

Statistics. The statistical significance in a difference between arithmetical means of test groups was assessed by unpaired t-test or Kruskal-Wallis test. After Kruskal-Wallis test, Scheffe's F-test was used as a post hoc test.
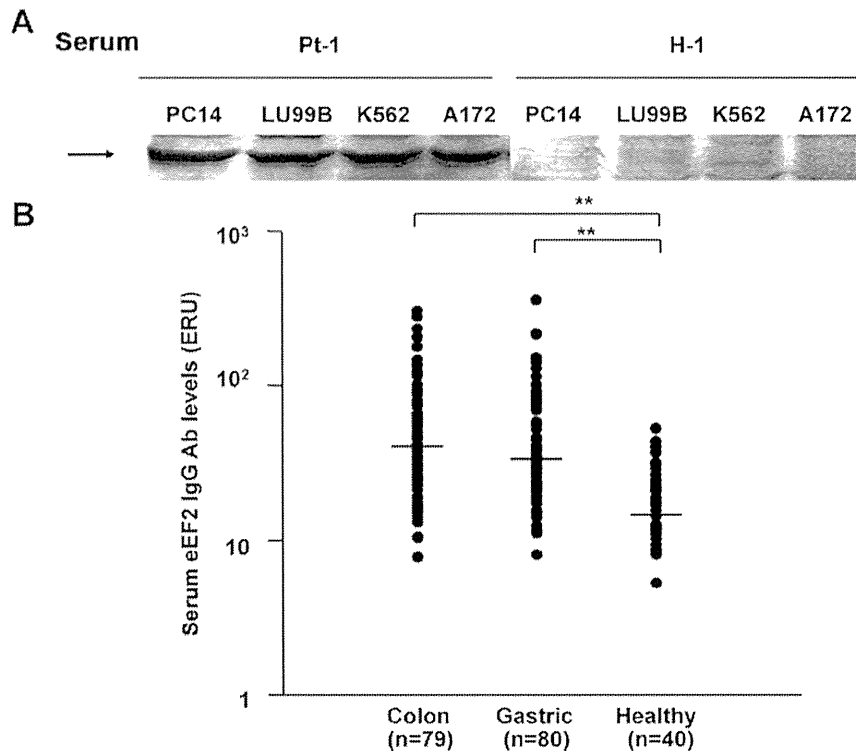
Figure 1. Elevation of serum eEF2 IgG autoantibody levels in cancer patients. (A) Cytoplasmic proteins from PC14, LU99B, K562 and A172 cells were subjected to immunoblot analysis using sera as the first antibodies. Representative results with sera from an HNSCC patient (Pt-1) and a healthy control individual (H-1) are shown. Arrows indicate the protein that is recognized by IgG autoantibody in the sera from the HNSCC patient. (B) Elevation of serum eEF2 IgG autoantibody levels in cancer patients. Assays were performed in duplicate. Colon, colorectal cancer; gastric, gastric cancer; and healthy, healthy individuals. Standard bar represents median value. **p<0.01. eEF2 Ab levels that produces the absorbance at 450 nm equal to that produced by 1 μg/ml of anti-eEF2 H-118 Ab in the ELISA system were defined as 1.0 eEF2-reacting-unit (ERU).

Results

Production of IgG autoantibody against eukaryotic elongation factor 2 (eEF2) in cancer patients. To identify novel tumor-associated antigens (TAAs) with high molecular weight (more than 100 kDa), which were difficult to isolate by standard two dimensional electrophoresis methods because they could not be absorbed into a strip gel, proteins from tumor lysates were first separated by SDS-PAGE, transferred to PVDF membrane, and then probed with sera from tumor-bearing patients. As shown in Fig. 1A, an approximately 100 kDa protein was recognized by sera from 4 of 10 HNSCC and 2 of 3 colon cancer patients in cytoplasmic proteins from two lung cell lines (PC14 and LU99B), one leukemic cell line (K562) and one glioblastoma cell line (A172), whereas it was not recognized by the sera from 5 healthy individuals. To identify this protein, cytoplasmic proteins of K562 cells were fractionated by density gradient isoelectric focusing, separated by SDS-PAGE, and subjected to immunoblot analysis using sera from an HNSCC patient as the first antibody. Since immunoblot analysis detected this protein in fractions of pH 6.62 and pH 6.75, the silver-stained band corresponding to this protein was excised from the SDS-PAGE gel and the protein was analyzed by MALDI-TOF Mass Spectrometry. The search for NCBInr database by MS-Fit software identified the protein as human eukaryotic elongation factor 2 (eEF2) that had M.W. of 95.3-kDa and calculated pI of 6.4.

Elevation of serum eEF2 IgG antibody levels in cancer patients. Serum eEF2 IgG Ab levels were examined by ELISA in 79 colorectal and 80 gastric cancer patients and 40 healthy individuals and detected in all the samples examined (Fig. 1B). eEF2 IgG Ab levels ranged from 7.8 to 301.7 (median 41.1), from 8.1 to 353.9 (median 33.6) and from 5.2 to 53.0 (median 20.6) ERU in colorectal and gastric cancer patients and healthy individuals, respectively. eEF2 IgG Ab levels were significantly (p<0.01) higher in both colorectal and gastric cancer patients than healthy individuals.

Overexpression of eEF2 in various types of human cancers. eEF2 protein was immunohistochemically examined in 51 lung cancers, 15 esophageal squamous cell carcinomas, 21 HNSCCs, 28 pancreatic cancers, 8 breast cancers, 16 glioblastoma multiformes, 4 prostate cancers and 50 NHLs. Immunohistochemical analysis with two different anti-EF2 antibodies recognizing different regions of eEF2 protein showed similar results. Overexpression of eEF2 protein was detected in 71.0% (22 of 31) of lung adenocarcinoma, 95.0% (19 of 20) of small-cell lung cancer, 73.3% (11 of 15) of esophageal cancer, 60.7% (17 of 28) of pancreatic cancer, 50.0% (4 of 8) of breast cancer, 75.0% (3 of 4) of prostate cancer, 52.4% (11 of 21) of HNSCC, 75.0% (12 of 16) of glioblastoma multiformes, and 94.0% (47 of 50) of NHL. Results are summarized in Table I. Representative results are shown in Fig. 2.

Table I. Overexpression of eEF2 in human cancers.

Cancer	Overexpression of eEF2 (%)
Lung cancer	80.4 (41/51)
Lung adenocarcinoma	71.0 (22/31)
Small cell lung cancer	95.0 (19/20)
Esophageal squamous cell carcinoma	73.3 (11/15)
Head and neck squamous cell carcinoma	52.4 (11/21)
Pancreatic cancer	60.7 (17/28)
Breast cancer	50.0 (4/8)
Glioblastoma	75.0 (12/16)
Prostate cancer	75.0 (3/4)
Non-Hodgkin's lymphoma	94.0 (47/50)
Diffuse large B cell lymphoma	92.5 (37/40)
Follicular lymphoma	100 (10/10)

Expression of eEF2 protein in human cancers was examined by immunohistochemistry. Immunostaining was evaluated as positive when cancer cells were stained brown in >10% of the cells.
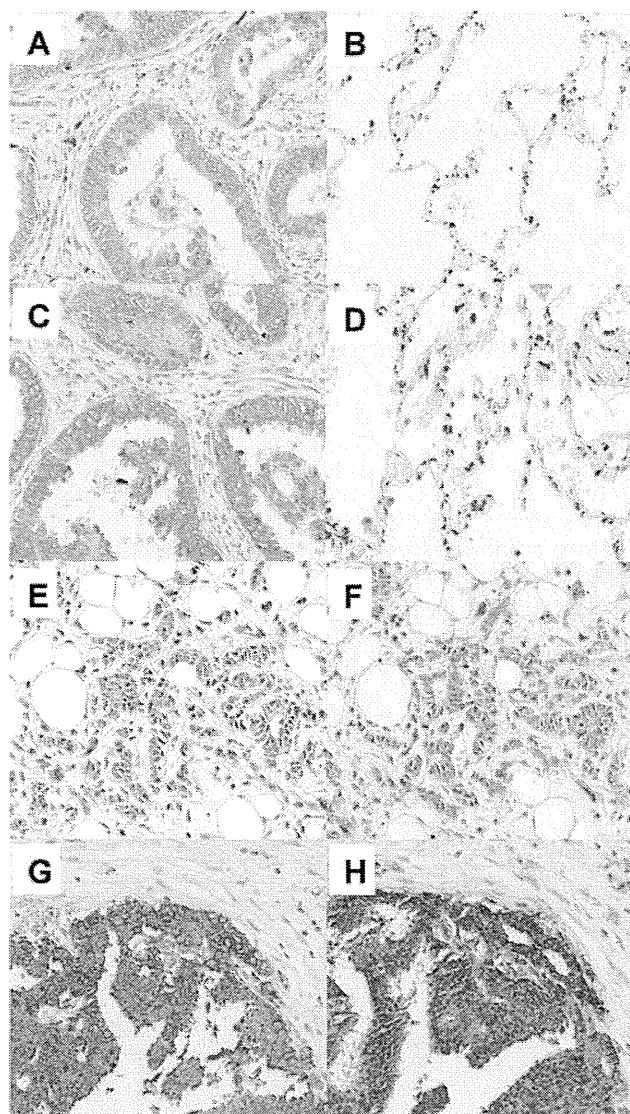

Figure 2. Overexpression of eEF2 in various types of cancers. Representative results of immunohistochemical analysis for eEF2 protein expression in (A and C) lung adenocarcinoma, (B and D) normal lung cells, (E and F) breast cancer, and (G and H) prostate cancer. eEF2 was stained with (A, B, E and G) eEF2-H118 antibody or (C, D, F and H) #SAB4500695 antibody. eEF2 protein was stained brown. Macrophages are non-specifically stained in normal lung tissues.

Overexpressed eEF2 gene is a non-mutated, wild-type. To examine whether or not the overexpressed *eEF2* gene was non-mutated, wild-type, the 5' (84-1334 nt) and the 3' (1314-2660 nt) sequences of eEF2 mRNA (coding sequence: 84-2660 nt) from five lung adenocarcinomas and five HNSCCs were amplified by RT-PCR and direct sequencing. No mutation was found in the *eEF2* gene in the 10 cancers examined (data not shown).

Knockdown of eEF2 inhibits cancer cell growth. To examine the role of eEF2 in cancer cell growth, either of two different shRNAs targeting eEF2 (shEF-1918 and shEF-2804) or a control shRNA targeting luciferase (shLuc) was transfected into four eEF2-expressing cells, lung cancer PC14, pancreatic cancer PCI6, fibrosarcoma HT-1080, and glioblastoma A172 and eEF2-undetectable breast cancer MCF7 cells. After culture for 72 h, both of the two shRNAs targeting eEF2 (shEF-1918 and shEF-2804) reduced eEF2 protein expression levels (Fig. 3A) and significantly inhibited cell growth in all the four eEF2-expressing cells examined (Fig. 3B). However, neither of the two shRNAs targeting eEF2 inhibited growth of eEF2-undetectable MCF7 cells.

*Identification of eEF2 peptides that bind to HLA-A*24:02 or HLA-A*02:01 molecules.* Epitope candidates of eEF2 that bound to HLA-A*24:02 or HLA-A*02:01 molecules were first analysed using ProPred-I computer algorithm (Table II).

As candidate epitope peptides that bound to HLA-A*24:02 molecules, EF78, EF786, EF701 and EF412 peptides were selected and analyzed for binding affinity to HLA-A*24:02 molecules by the MHC stabilization assay. These peptides were pulsed to T2-2402 cells and the expression of HLA-A*24:02 molecules on the cell surface was analyzed by flow cytometry. As shown in Table II, all the four peptides increased the expression of HLA-A24:02 molecules on T2-2402 cells as a result of the stabilization of HLA-A24:02

molecules. Among the four peptides, EF786 peptide showed binding affinity higher than $CMVpp65_{328-336}$, which was an exogenous cytomegalovirus antigen epitope, to the HLA-A*24:02 molecules. As candidate peptides that bound to HLA-A*02:01 molecules, EF292, EF739, EF519 and EF671 peptides were selected and analyzed for binding affinity to HLA-A*02:01 molecules by the MHC stabilization assay. As shown in Table II, all the four peptides increased the expression of HLA-A02:01 molecules on T2-0201 cells and EF292 peptide showed the highest binding affinity to HLA-A*02:01 molecules among the four HLA-A*02:01-binding peptides examined.

*Generation of EF2-specific CTLs from HLA-A*24:02- or HLA-A*02:01-positive donors.* Treg-depleted PBMCs from

Table II. Characteristics of EF2-derived peptides and results of the MHC stabilization assay.

Peptide	Position (aa)	Sequence	Score	%MFI increase
HLA-A*24:02-binding peptides				
EF78	78-86	FYELSENDL	360	40.5
EF786	786-794	AYLPVNESF	252	1552.1
EF701	701-709	RFDVHDVTL	40	297.3
EF412	412-420	AFGRVFSGL	33.6	47.9
CMVpp65 328-336		QYDPVAALF		1344.1
HLA-A*02:01-binding peptides				
EF292	292-300	LILDPIFKV	3290	183.3
EF739	739-747	RLMEPIYLV	2426	141.1
EF519	519-527	KLVEGLKRL	705	58.9
EF671	671-679	YLNEIKDSV	642	89.6

The primary amino acid sequences of human eEF2 were analyzed for consensus motifs for 9-mer peptides capable of binding to HLA-A*24:02 or 02:01 molecules using ProPred-I software. Percentage MFI increase in MHC stabilization assay was calculated as follows: percentage MFI increase = (MFI with the given peptide - MFI without peptide)/(MFI without peptide) x 100.
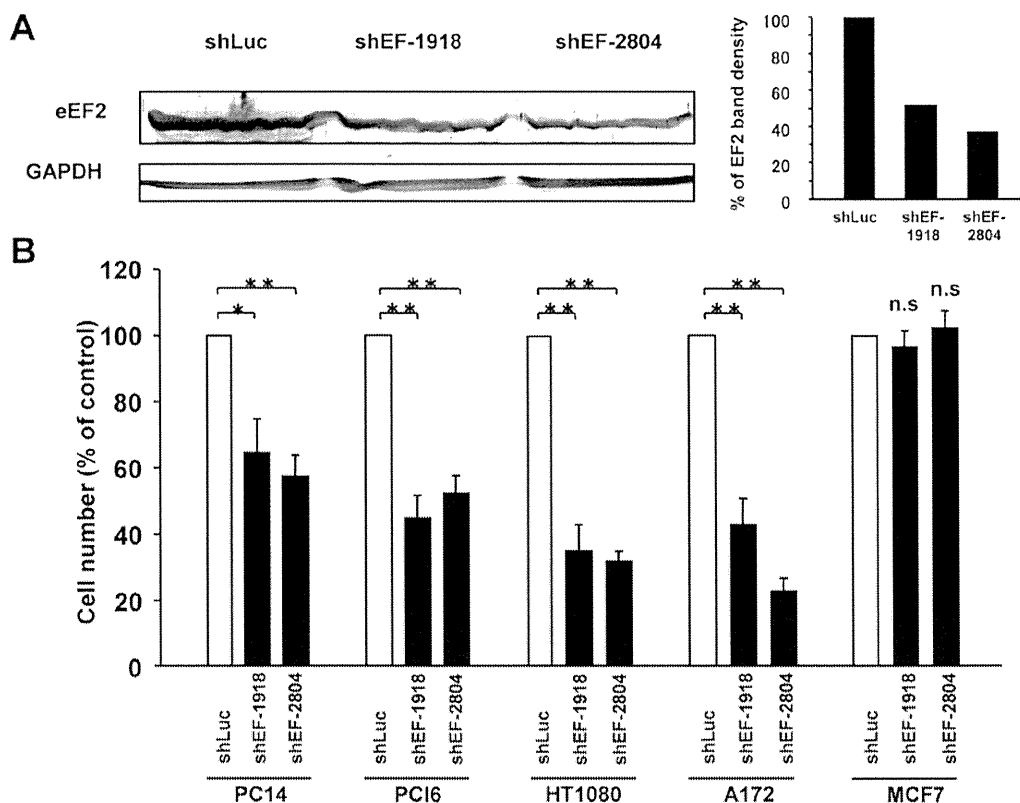

Figure 3. Knockdown of eEF2 inhibits cancer cell growth. Two shRNA vectors targeting different sequences of eEF2 (shEF-1918 and shEF-2804 targeting 1918-1947 and 2804-2833 nt of eEF2 sequence, respectively) or control shRNA targeting luciferase (shLuc) was transfected into PC14, PCI6, HT1080, A172 and MCF7 cells. (A) Reduction in eEF2 protein expression levels in HT1080 cells. Results of western blot analysis are shown. (B) After 72 h of transfection, the cell numbers were examined. *p<0.05; **p<0.01. Experiments were independently performed three times.

HLA-A*24:02- or HLA-A*02:01-positive healthy donors were repeatedly stimulated with EF2 peptides (EF786 and EF292 peptides for HLA-A*24:02- and HLA-A*02:01-positive healthy donors, respectively) and pulsed irradiated autologous DCs and EF2 peptide-specific CTLs were established.

To examine whether EF2 peptides are capable of eliciting CTL responses, CTL activities of established CTLs were examined. As shown in Fig. 4A, EF786-specific, HLA-A*24:02-restricted CTLs lysed EF786 peptide-pulsed T2-2402 cells but not unpulsed ones. The EF786-specific

Table III. Characteristics of target cells in the killing assay.

Target cells	HLA-A*24:02 expression	HLA-A*02:01 expression	eEF2 expression
T2	-	-	Undetectable
T2-2402	+	-	Undetectable
T2-0201	-	+	Undetectable
SW480	+		+
AZ-521	-		+
MKN28	-		+
TF-1		+	+
K562	-	-	+
MCF7		+	Undetectable

Cell surface protein expression of HLA-A molecules was confirmed by flow cytometry. Expression of eEF2 protein was analyzed by western blot analysis.
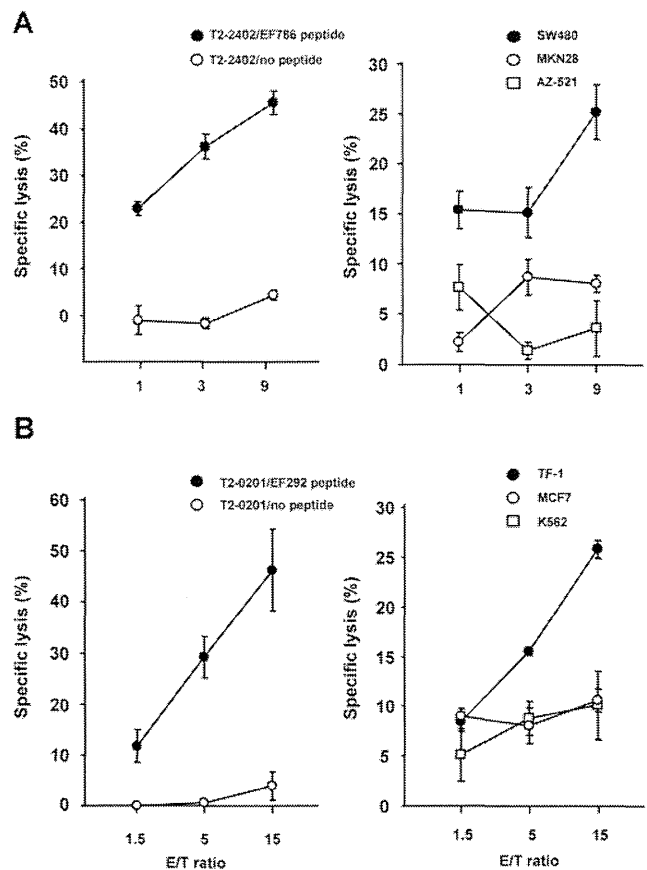

Figure 4. Generation of eEF2-specific CTLs. (A, left panel) Specific lysis of EF786 peptide-pulsed T2-2402 cells by EF786-specific, HLA-A*24:02-restricted CTLs. (A, right panel) Specific lysis of eEF2-expressing, HLA-A*24:02-positive SW480 by EF786-specific, HLA-A*24:02-restricted CTLs. AZ-521 and MKN28 are eEF2-expressing, but HLA-A*24:02-negative. (B, left panel) Specific lysis of EF292 peptide-pulsed T2-0201 cells by EF292-specific, HLA-A*02:01-restricted CTLs. (B, right panel) Specific lysis of eEF2-expressing, HLA-A*02:01-positive TF-1 cells by EF292-specific, HLA-A*02:01-restricted CTLs. K562 is eEF2-expressing and HLA-A*02:01-negative, and MCF7 is eEF2-undetectable and HLA-A*02:01-positive. E/T, effector/target ratio. CTL cytotoxic assays were performed in triplicate.

CTLs lysed HLA-A*24:02-positive, eEF2-expressing SW480 cells, but not HLA-A*24:02-negative, eEF2-expressing AZ-521 and MKN28 cells. As shown in a Fig. 4B, EF292 peptide-specific, HLA-A*02:01-restricted CTLs lysed EF292 peptide-pulsed T2-0201 cells but not unpulsed ones. Moreover, the EF292-specific CTLs lysed HLA-A*02:01-positive, eEF2-expressing TF-1 cells, but not HLA-A*02:01-negative, eEF2-expressing K562 cells and HLA-A*02:01-positive, eEF2-undetectable MCF7 cells (Fig. 4B).

Discussion

We showed that eEF2 was overexpressed in the majority of various types of tumors such as lung, esophageal, pancreatic, and breast cancer and promoted growth of various types of cancer cells. Moreover, *eEF2* gene product elicited both humoral and cellular eEF2-specific immune responses. The production of eEF2 IgG autoantibody was enhanced in patients with colorectal and gastric cancer and 9-mer eEF2 peptides elicited EF2-specific CTLs from healthy donors. These results indicated that overexpressed eEF2 played an oncogenic role and served as a TAA in these tumors.

It is considered that production of autoantibody indicates the potential of its antigen as a target of cancer immunotherapy (20). In the present study, we showed the elevation of serum EF2 IgG levels in colorectal and gastric cancer patients, indicating that eEF2 overexpressed in cancer cells was recognized by the host immune system and induced eEF2-specific immune responses. Since production of IgG autoantibody needed help from CD4+ helper T cells (Th cells) for class switch from IgM to IgG, elevation of EF2 IgG Ab levels indicated the activation of EF2-specific Th cells. It is well established that Th cells play an important role in the immune responses against cancer (21). CD4+ Th cells are required for activation and maintenance of CD8+ CTLs, but they could also exert cytotoxic function against cancer in the absence of CD8+ CTLs recognizing antigenic peptides presented by MHC class II molecules (22,23). These results indicated that EF2 protein was an immunogenic molecule

that is capable of eliciting not only humoral but also cellular immune responses. In fact, eEF2-derived EF786 peptide showed the binding affinity higher than CMVpp65328-336, an exogenous viral antigen epitope, and elicited *in vitro* EF786-specific CTLs from PBMCs of HLA-A*24:02-positive healthy donors. Taken together, eEF2 protein is highly immunogenic and a promising target molecule for cancer immunotherapy.

Expression of target molecules in tumor cells is the first requisite for TAA-targeting cancer immunotherapy. Survivin is a member of the family of the inhibitor of apoptosis proteins and functions as a key regulator of mitosis and programmed cell death (24). Survivin is overexpressed in various types of tumors with the frequency of 34.5% in gastric cancers (25), 50-60% in colorectal cancers (25,26), 64% in malignant gliomas (27), 53-72% in lung cancers (28,29), and 70.7% in breast cancers (30). Cancer vaccines to induce an antigen-specific immune responses against survivin-expressing tumor cells have been developed with

promising results (31,32). Thus, survivin appears to be a promising TAA. However, survivin-targeted immunotherapy may be applicable to a limited population of patients because of its low expression rates in several tumors. In addition, the frequency of survivin-positive tumor cells may vary in individual tumors (25). Thus, the existence of tumor cells lacking survivin could result in tumor evasion from CTL responses against survivin induced by vaccination. NY-ESO-1 is a member of cancer testis antigens and is expressed in a variety of common cancers. Clinical trials that evaluate therapeutic responses against NY-ESO-1 are underway in various cancers (33). However, NY-ESO-1 protein was expressed in only 20 to 30% of lung (34), bladder and ovarian cancers (35) and melanoma and was undetectable in colon and renal cancers (36). Thus, therapeutic strategy against NY-ESO-1 is applicable to a minor population of cancer patients. Compared to these TAAs, eEF2 is more attractive as a target molecule of cancer immunotherapy because of its high frequency of overexpression in various types of cancers. The frequency of eEF2 overexpression exceeded 70% in lung, esophageal, breast and prostate cancers, and 90% in gastric and colorectal cancers and NHL, as shown in the present and previous (14) studies. These results indicated that eEF2-targeted immunotherapy should be a therapeutic strategy that would be applicable to the majority of cancer patients. WT1 is also a promising target molecule of immunotherapy and was ranked as top of TAAs (37). WT1 is overexpressed in the majority of leukemia (38) and various types of tumors such as lung (39), colorectal (40) and pancreatic cancer (41), and glioblastoma multiforme (42). However, WT1 might be less expressed in malignant lymphoma. In diffuse large B-cell lymphoma the most common type of NHL, WT1 protein was detected in only 33% of the cases examined (43). Thus, eEF2-targeted immunotherapy may have a priority for NHL.

One mechanism for escape from immune surveillance is the loss of expression of target molecules in cancer cells (44). Therefore, it is important to know whether or not loss of eEF2 expression affects tumor growth in consideration of the potential of eEF2 as a target molecule for cancer immmunotherapy. As shown in the present study, knockdown of eEF2 by shRNA significantly inhibited cancer cell growth. Also, we have demonstrated that eEF2 was overexpressed in the majority of gastric and colorectal cancers and promoted progression of G_2/M in the cell cycle, resulting in the enhancement of *in vitro* and *in vivo* cancer cell growth (14). Based on these findings showing the involvement of eEF2 in cancer cell growth, it is unlikely that antigenic loss of eEF2 could become a mechanism of tumor escape from eEF2-specific immune responses.

A primary goal of cancer immunotherapy is generation of effective CTL responses through the expansion of robust pre-existing, naturally occurring CD8^{+} CTL precursors and the establishment of long-lasting memory CD8^{+} T cells. This critically depends on the activation of pre-existing antigen-specific CTL precursors as the initial step to induce immune responses. In the present study, eEF2-specific CTL clones were established from HLA-A[*]24:02- or HLA-A[*]02:01-positive healthy donors. In addition, eEF2 IgG autoantibody is detected at low levels in healthy individuals examined. Since these results indicated the existence of not only eEF2-specific CTL precursors but also eEF2-specific B and Th cells even in healthy donors without cancer, the host immune system of cancer patients should have a potential to make robust immune responses against eEF2-expressing cancers by vaccination with EF2 protein or peptide.

In conclusion, eEF2 that is overexpressed in a wide variety of cancers is a promising cancer antigen that can elicit both humoral and cellular immune responses and shows promise as a target molecule of cancer immunotherapy.

Acknowledgements

References

1. Lesterhuis WJ, Haanen JB and Punt CJ: Cancer immunotherapy - revisited. Nat Rev Drug Discov 10: 591-600, 2011.
2. Wright SE: Immunotherapy of breast cancer. Expert Opin Biol Ther 12: 479-490, 2012.
3. Slingluff CL Jr: The present and future of peptide vaccines for cancer: single or multiple, long or short, alone or in combination? Cancer J 17: 343-350, 2011.
4. Murala S, Alli V, Kreisel D, Gelman AE and Krupnick AS: Current status of immunotherapy for the treatment of lung cancer. J Thorac Dis 2: 237-244, 2010.
5. Topalian SL, Weiner GJ and Pardoll DM: Cancer immunotherapy comes of age. J Clin Oncol 29: 4828-4836, 2011.
6. Desmetz C, Mange A, Maudelonde T and Solassol J: Autoantibody signatures: progress and perspectives for early cancer detection. J Cell Mol Med 15: 2013-2024, 2011.
7. Murphy MA, O'Leary JJ and Cahill DJ: Assessment of the humoral immune response to cancer. J Proteomics 75: 4573-4579, 2012.
8. Grzmil M and Hemmings BA: Translation regulation as a therapeutic target in cancer. Cancer Res 72: 3891-3900, 2012.
9. Bilanges B and Stokoe D: Mechanism of translational deregulation in human tumors and therapeutic intervention strategies. Oncogene 26: 5973-5990, 2007.
10. Hizli AA, Chi Y, Swanger J, Carter JH, Liao Y, Welcker M, Ryazanov AG and Clurman BE: Phosphorylation of eukaryotic elongation factor 2 (eEF2) by cyclin A-cyclin-dependent kinase 2 regulates its inhibition by eEF2 kinase. Mol Cell Biol 33: 596-604, 2013.
11. White SJ, Kasman LM, Kelly MM, Lu P, Spruill L, McDermott PJ and Voelkel-Johnson C: Doxorubicin generates a proapoptotic phenotype by phosphorylation of EF-2. Free Radic Biol Med 43: 1313-1321, 2007.
12. Kruiswijk F, Yuniati L, Magliozzi R, Low TY, Lim R, Bolder R, Mohammed S, Proud CG, Heck AJ, Pagano M and Guardavaccaro D: Coupled activation and degradation of eEF2K regulates protein synthesis in response to genotoxic stress. Sci Signal 5: ra40, 2012.
13. Schwer CI, Stoll P, Rospert S, Fitzke E, Schallner N, Burkle H, Schmidt R and Humar M: Carbon monoxide releasing molecule-2 CORM-2 represses global protein synthesis by inhibition of eukaryotic elongation factor eEF2. Int J Biochem Cell Biol 45: 201-212, 2013.
14. Nakamura J, Aoyagi S, Nanchi I, Nakatsuka S, Hirata E, Shibata S, Fukuda M, Yamamoto Y, Fukuda I, Tatsumi N, Ueda T, Fujiki F, Nomura M, Nishida S, Shirakata T, Hosen N, Tsuboi A, Oka Y, Nezu R, Mori M, Doki Y, Aozasa K, Sugiyama H and Oji Y: Overexpression of eukaryotic elongation factor eEF2 in gastrointestinal cancers and its involvement in G_2/M progression in the cell cycle. Int J Oncol 34: 1181-1189, 2009.

15. Kuzushima K, Hayashi N, Kimura H and Tsurumi T: Efficient identification of HLA-A*2402-restricted cytomegalovirus-specific CD8(+) T-cell epitopes by a computer algorithm and an enzyme-linked immunospot assay. Blood 98: 1872-1881, 2001.

16. Oka Y, Elisseeva OA, Tsuboi A, Ogawa H, Tamaki H, Li H, Oji Y, Kim EH, Soma T, Asada M, Ueda K, Maruya E, Saji H, Kishimoto T, Udaka K and Sugiyama H: Human cytotoxic T lymphocyte responses specific for peptides of wild-type Wilms' tumor gene WT1 product. Immunogenetics 51: 99-107, 2000.

17. Masuda T, Ide N and Kitabatake N: Effects of chemical modification of lysine residues on the sweetness of lysozyme. Chem Senses 30: 253-264, 2005.

18. Oji Y, Kitamura Y, Kamino E, Kitano A, Sawabata N, Inoue M, Mori M, Nakatsuka S, Sakaguchi N, Miyazaki K, Nakamura M, Fukuda I, Nakamura J, Tatsumi N, Takakuwa T, Nishida S, Shirakata T, Hosen N, Tsuboi A, Nezu R, Maeda H, Oka Y, Kawase I, Aozasa K, Okumura M, Miyoshi S and Sugiyama H: WT1 IgG antibody for early detection of nonsmall cell lung cancer and as its prognostic factor. Int J Cancer 125: 381-387, 2009.

19. Morishima S, Akatsuka Y, Nawa A, Kondo E, Kiyono T, Torikai H, Nakanishi T, Ito Y, Tsujimura K, Iwata K, Ito K, Kodera Y, Morishima Y, Kuzushima K and Takahashi T: Identification of an HLA-A24-restricted cytotoxic T lymphocyte epitope from human papillomavirus type-16 E6: the combined effects of bortezomib and interferon-gamma on the presentation of a cryptic epitope. Int J Cancer 120: 594-604, 2007.

20. Chiriva-Internati M, Yu Y, Mirandola L, D'Cunha N, Hardwicke F, Cannon MJ, Cobos E and Kast WM: Identification of AKAP-4 as a new cancer/testis antigen for detection and immunotherapy of prostate cancer. Prostate 72: 12-23, 2012.

21. Qin Z and Blankenstein T: CD4+ T cell-mediated tumor rejection involves inhibition of angiogenesis that is dependent on IFNγ receptor expression by nonhematopoietic cells. Immunity 12: 677-686, 2000.

22. Bogen B, Munthe L, Sollien A, Hofgaard P, Omholt H, Dagnaes F, Dembic Z and Lauritzsen GF: Naive CD4+ T cells confer idiotype-specific tumor resistance in the absence of antibodies. Eur J Immunol 25: 3079-3086, 1995.

23. Lin Y, Fujiki F, Katsuhara A, Oka Y, Tsuboi A, Aoyama N, Tanii S, Nakajima H, Tatsumi N, Morimoto S, Tamanaka T, Tachino S, Hosen N, Nishida S, Oji Y, Kumanogoh A and Sugiyama H: HLA-DPB1*05:01-restricted WT1 332-specific TCR-transduced CD4+ T lymphocytes display a helper activity for WT1-specific CTL induction and a cytotoxicity against leukemia cells. J Immunother 36: 159-170, 2013.

24. Mita AC, Mita MM, Nawrocki ST and Giles FJ: Survivin: key regulator of mitosis and apoptosis and novel target for cancer therapeutics. Clin Cancer Res 14: 5000-5005, 2008.

25. Lu CD, Altieri DC and Tanigawa N: Expression of a novel anti-apoptosis gene, survivin, correlated with tumor cell apoptosis and p53 accumulation in gastric carcinomas. Cancer Res 58: 1808-1812, 1998.

26. Kawasaki H, Altieri DC, Lu CD, Toyoda M, Tenjo T and Tanigawa N: Inhibition of apoptosis by survivin predicts shorter survival rates in colorectal cancer. Cancer Res 58: 5071-5074, 1998.

27. Chakravarti A, Noll E, Black PM, Finkelstein DF, Finkelstein DM, Dyson NJ and Loeffler JS: Quantitatively determined survivin expression levels are of prognostic value in human gliomas. J Clin Oncol 20: 1063-1068, 2002.

28. Wang M, Liu BG, Yang ZY, Hong X and Chen GY: Significance of survivin expression: Prognostic value and survival in stage III non-small cell lung cancer. Exp Ther Med 3: 983-988, 2012.

29. Bria E, Visca P, Novelli F, Casini B, Diodoro MG, Perrone-Donnorso R, Botti C, Sperduti I, Facciolo F, Milella M, Cecere FL, Cognetti F and Mottolese M: Nuclear and cyto-plasmic cellular distribution of survivin as survival predictor in resected non-small-cell lung cancer. Eur J Surg Oncol 34: 593-598, 2008.

30. Tanaka K, Iwamoto S, Gon G, Nohara T, Iwamoto M and Tanigawa N: Expression of survivin and its relationship to loss of apoptosis in breast carcinomas. Clin Cancer Res 6: 127-134, 2000.

31. Idenoue S, Hirohashi Y, Torigoe T, Sato Y, Tamura Y, Hariu H, Yamamoto M, Kurotaki T, Tsuruma T, Asanuma H, Kanaseki T, Ikeda H, Kashiwagi K, Okazaki M, Sasaki K, Sato T, Ohmura T, Hata F, Yamaguchi K, Hirata K and Sato N: A potent immuno-genic general cancer vaccine that targets survivin, an inhibitor of apoptosis proteins. Clin Cancer Res 11: 1474-1482, 2005.

32. Kameshima H, Tsuruma T, Torigoe T, Takahashi A, Hirohashi Y, Tamura Y, Tsukahara T, Ichimiya S, Kanaseki T, Iwayama Y, Sato N and Hirata K: Immunogenic enhancement and clinical effect by type-I interferon of anti-apoptotic protein, survivin-derived peptide vaccine, in advanced colorectal cancer patients. Cancer Sci 102: 1181-1187, 2011.

33. Cebon J, Knights A, Ebert L, Jackson H and Chen W: Evaluation of cellular immune responses in cancer vaccine recipients: lessons from NY-ESO-1. Expert Rev Vaccines 9: 617-629, 2010.

34. Kim SH, Lee S, Lee CH, Lee MK, Kim YD, Shin DH, Choi KU, Kim JY, Park do Y and Sol MY: Expression of cancer-testis antigens MAGE-A3/6 and NY-ESO-1 in non-small-cell lung carcinomas and their relationship with immune cell infiltration. Lung 187: 401-411, 2009.

35. Yakirevich E, Sabo E, Lavie O, Mazareb S, Spagnoli GC and Resnick MB: Expression of the MAGE-A4 and NY-ESO-1 cancer-testis antigens in serous ovarian neoplasms. Clin Cancer Res 9: 6453-6460, 2003.

36. Jungbluth AA, Chen YT, Stockert E, Busam KJ, Kolb D, Iversen K, Coplan K, Williamson B, Altorki N and Old LJ: Immunohistochemical analysis of NY-ESO-1 antigen expression in normal and malignant human tissues. Int J Cancer 92: 856-860, 2001.

37. Cheever MA, Allison JP, Ferris AS, Finn OJ, Hastings BM, Hecht TT, Mellman I, Prindiville SA, Viner JL, Weiner LM and Matrisian LM: The prioritization of cancer antigens: a national cancer institute pilot project for the acceleration of translational research. Clin Cancer Res 15: 5323-5337, 2009.

38. Inoue K, Sugiyama H, Ogawa H, Nakagawa M, Yamagami T, Miwa H, Kita K, Hiraoka A, Masaoka T, Nasu K, Kyo T, Dohy H, Nakauchi H, Ishidate T, Akiyama T and Kishimoto T: WT1 as a new prognostic factor and a new marker for the detection of minimal residual disease in acute leukemia. Blood 84: 3071-3079, 1994.

39. Oji Y, Miyoshi S, Maeda H, Hayashi S, Tamaki H, Nakatsuka S, Yao M, Takahashi E, Nakano Y, Hirabayashi H, Shintani Y, Oka Y, Tsuboi A, Hosen N, Asada M, Fujioka T, Murakami M, Kanato K, Motomura M, Kim EH, Kawakami M, Ikegame K, Ogawa H, Aozasa K, Kawase I and Sugiyama H: Overexpression of the Wilms' tumor gene WT1 in de novo lung cancers. Int J Cancer 100: 297-303, 2002.

40. Oji Y, Yamamoto H, Nomura M, Nakano Y, Ikeba A, Nakatsuka S, Abeno S, Kiyotoh E, Jomgeow T, Sekimoto M, Nezu R, Yoshikawa Y, Inoue Y, Hosen N, Kawakami M, Tsuboi A, Oka Y, Ogawa H, Souda S, Aozasa K, Monden M and Sugiyama H: Overexpression of the Wilms' tumor gene WT1 in colorectal adenocarcinoma. Cancer Sci 94: 712-717, 2003.

41. Oji Y, Nakamori S, Fujikawa M, Nakatsuka S, Yokota A, Tatsumi N, Abeno S, Ikeba A, Takashima S, Tsujie M, Yamamoto H, Sakon M, Nezu R, Kawano K, Nishida S, Ikegame K, Kawakami M, Tsuboi A, Oka Y, Yoshikawa K, Aozasa K, Monden M and Sugiyama H: Overexpression of the Wilms' tumor gene WT1 in pancreatic ductal adenocarcinoma. Cancer Sci 95: 583-587, 2004.

42. Oji Y, Suzuki T, Nakano Y, Maruno M, Nakatsuka S, Jomgeow T, Abeno S, Tatsumi N, Yokota A, Aoyagi S, Nakazawa T, Ito K, Kanato K, Shirakata T, Nishida S, Hosen N, Kawakami M, Tsuboi A, Oka Y, Aozasa K, Yoshimine T and Sugiyama H: Overexpression of the Wilms' tumor gene WT1 in primary astro-cytic tumors. Cancer Sci 95: 822-827, 2004.

43. Drakos E, Rassidakis GZ, Tsioli P, Lai R, Jones D and Medeiros LJ: Differential expression of WT1 gene product in non-Hodgkin lymphomas. Appl Immunohistochem Mol Morphol 13: 132-137, 2005.

44. Schreiber RD, Old LJ and Smyth MJ: Cancer immuno-editing: integrating immunity's roles in cancer suppression and promotion. Science 331: 1565-1570, 2011.

Histamine Contributes to Tissue Remodeling via Periostin Expression

Lingli Yang[1], Hiroyuki Murota[1], Satoshi Serada[2], Minoru Fujimoto[2], Akira Kudo[3], Tetsuji Naka[2] and Ichiro Katayama[1]

Histamine is thought to have a critical role in the synthesis of extracellular matrix in skin and may be involved in tissue remodeling of allergic diseases. Recent studies revealed that periostin, a matricelluar protein, contributed to tissue remodeling; however, a link between periostin and histamine remains unproven. We investigated whether periostin was involved in histamine-induced collagen production. Cultured dermal fibroblasts derived from wild-type (WT) or periostin knockout ($PN^{-/-}$) mice were stimulated with histamine, and then collagen and periostin production was evaluated. Histamine induced collagen gene expression in WT fibroblasts in the late phase but not in the early phase, whereas no effect on collagen expression was observed in histamine-stimulated $PN^{-/-}$ fibroblasts. In WT fibroblasts, histamine directly induced periostin expression in a dose-dependent manner, and an H1 receptor antagonist blocked both periostin and collagen expression. Histamine activated extracellular signal-regulated kinase 1/2 (ERK1/2) through the H1 receptor. Periostin induction was inhibited by either H1 antagonist or ERK1/2 inhibitor treatment in vitro and was attenuated in $H1R^{-/-}$ mice. Elevated expression of periostin was found in lesional skin from atopic dermatitis patients. These results suggest that histamine mediates periostin induction and collagen production through activation of the H1 receptor–mediated ERK1/2 pathway; furthermore, histamine may accelerate the chronicity of atopic dermatitis.

INTRODUCTION

Tissue remodeling is both a cause and a consequence of allergic inflammation and is considered a target for therapeutic intervention.

Understanding the underlying mechanisms that cause tissue remodeling is progressing gradually, and certain factors that are correlated with allergic inflammation have been found to be involved in tissue remodeling. Among them, histamine has been found to induce de novo synthesis of collagen from fibroblasts in both in vivo and in vitro experiments (Sandberg, 1962, 1964; Cohen et al., 1972; Murota et al., 2008). Furthermore, it is well known that antihistamine drugs used for the treatment of allergic disorders improve hypertrophic scars (Murakami et al., 1998). These results indicate that histamine may be involved in the mechanism of tissue

remodeling in allergic diseases; however, it remains unknown how histamine contributes to tissue remodeling.

Recent studies showed that expression of periostin, a matricellular protein with profibrogenic function, increased in sera and lesional tissue from patients with allergic diseases, such as allergic rhinitis, asthma, and atopic dermatitis (AD), and that this expression was associated with airway or other tissue remodeling (Takayama et al., 2006; Hur et al., 2012; Masuoka et al., 2012). Furthermore, periostin has also emerged as a key regulator in the development of wound healing and scleroderma (Ontsuka et al., 2012; Yang et al., 2012). To the best of our knowledge, the impact of histamine on the expression level of periostin is unknown. Therefore, in this study, we investigated the correlation between histamine and the fibrotic factor periostin in primary cultured dermal fibroblasts.

[1]Department of Dermatology, Osaka University Graduate School of Medicine, Osaka, Japan; [2]Laboratory for Immune Signal, National Institute of Biomedical Innovation, Osaka, Japan and [3]Department of Biological Information, Tokyo Institute of Technology, Yokohama, Japan

Correspondence: Hiroyuki Murota, Department of Dermatology, Osaka University Graduate School of Medicine, 2-2 Yamadaoka, Suita 565-0871, Osaka, Japan. E-mail: h-murota@derma.med.osaka-u.ac.jp

RESULTS

Collagen production is induced by histamine stimulation

To investigate whether histamine influences collagen synthesis, primary cultured murine dermal fibroblasts were stimulated with histamine at concentrations ranging from 0 to 100 μM, as described in our previous report (Murota et al., 2008; Murota and Katayama, 2009).

Histamine-induced type I collagen production was observed with concentrations of histamine from 1 to 100 μM (Figure 1). Compared with nontreated controls, collagen synthesis was significantly increased after histamine treatment
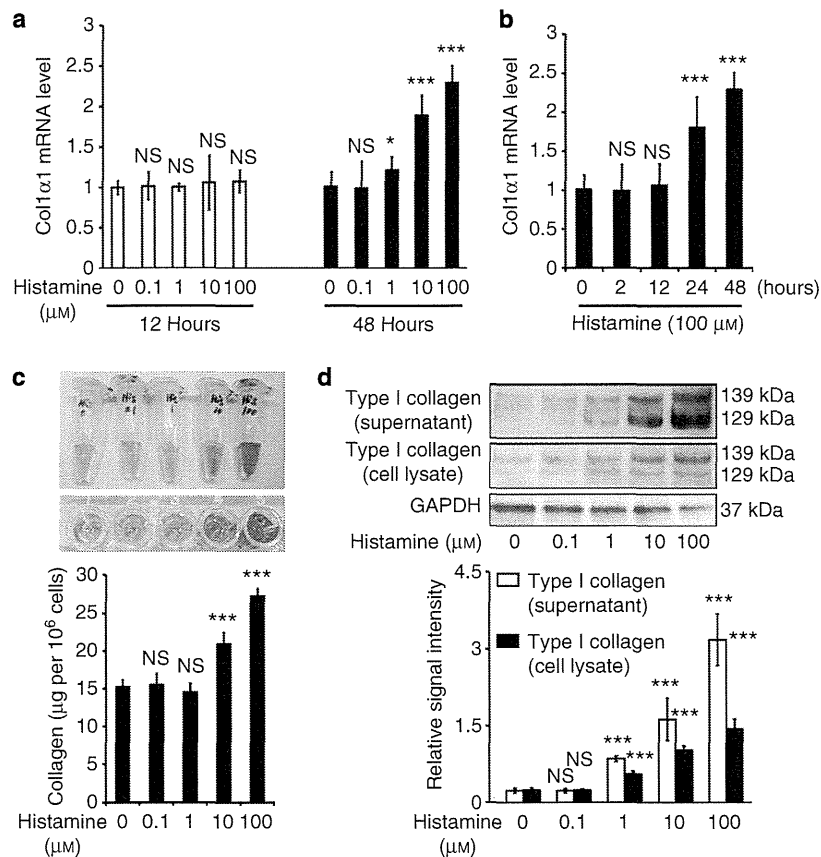
Figure 1. Collagen production is induced by histamine stimulation in cultured wild-type (WT) fibroblasts. (a) Effect of histamine on collagen type-I alpha 1 (Col1α1) mRNA expression was assessed by quantitative real-time reverse transcriptase–PCR (qRT-PCR) at 12 hours (white bar) and 48 hours (black bar) after the addition of histamine at the indicated concentration. (b) Effect of histamine on Col1α1 mRNA expression after the stimulation with histamine (100 μM) for the indicated time periods. (c) Soluble collagen content in the supernatants of WT fibroblasts that had been stimulated with histamine for 48 hours. (d) Representative western blotting and quantitative analyses of signal density on blots from three independent experiments analyzing collagen protein expression in response to 48 hours of histamine stimulation (using glyceraldehyde 3-phosphate dehydrogenase (GAPDH) as an internal control). Values were derived from three independent experiments using WT fibroblast cultures. Values represent the mean ± SD for the three independent experiments in each condition. *$P < 0.05$; ***$P < 0.001$; NS, no significance, compared with control (0 μM histamine) by one-way analysis of variance (ANOVA) followed by Dunnett's test.

in a dose-dependent manner (Figure 1a, c and d). No significant increase was observed at 2 and 12 hours, whereas collagen was markedly induced by histamine 24 and 48 hours after addition (Figure 1a and b). In our previous study (Yang *et al.*, 2012), the mRNA expression of type I collagen was found to be significantly increased in cultured mouse dermal fibroblasts after a 2-hour stimulation with recombinant periostin alone. Therefore, these late responses in the present study may be a result of *de novo* synthesis of certain second messengers.

Periostin is upregulated upon histamine stimulation in dermal fibroblasts

Next, to investigate whether histamine affects the expression level of periostin, we stimulated wild-type (WT) primary dermal fibroblasts with histamine at the indicated concentrations (Figure 2). As expected, two hours of incubation with histamine produced a significant dose-dependent increase of

periostin mRNA expression in dermal fibroblasts, as assessed by reverse transcriptase–PCR and quantitative real-time reverse transcriptase–PCR (Figure 2a and b). After 24 hours of incubation with histamine, the periostin protein levels increased in the culture supernatant and cell lysates (Figure 2 c). These results suggest that histamine may directly upregulate the transcription and synthesis of periostin.

Histamine upregulates periostin expression via histamine receptor 1 (H1R)

To identify the histamine receptor subtype responsible for the histamine-induced periostin expression, antagonists for H1R, H2R, and H4R were tested *in vitro*. The effects of histamine on periostin mRNA and protein levels were evaluated at 2 hours or 24 hours, respectively, in dermal fibroblasts after histamine stimulation following preincubation with or without these histamine receptor antagonists (Figure 3a and b). Histamine-induced periostin expression was blocked by H1R antagonist
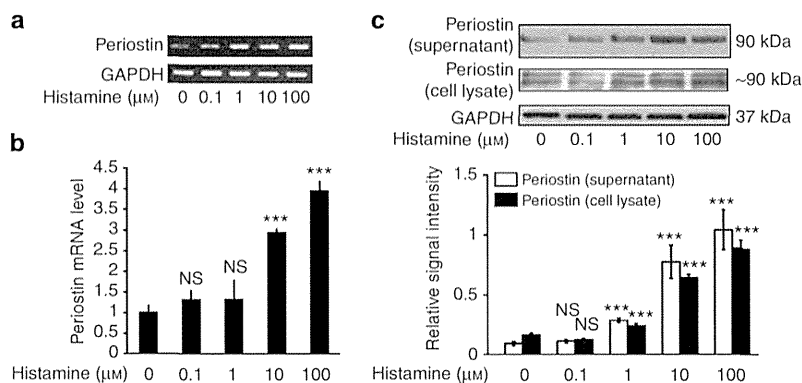
Figure 2. Periostin is upregulated upon histamine stimulation in cultured wild-type (WT) fibroblasts. WT fibroblasts were stimulated with histamine at the indicated concentrations for 2 hours (a, b) or 24 hours (c). Periostin mRNA expression was determined by reverse transcriptase–PCR (RT-PCR) analysis (a) and real-time PCR analysis (b). Periostin protein expression was evaluated by western blotting analysis (c). Three independent experiments were performed, and representative blots and quantitative analysis of signal density on blots from three independent experiments are shown (using glyceraldehyde 3-phosphate dehydrogenase (GAPDH) as an internal control). Values in b and c are shown as mean ± SD for three independent experiments. ***$P<0.001$; NS, no significance, compared with control (0 μM histamine) by one-way analysis of variance (ANOVA) followed by Dunnett's test.

but not by either H2R or H4R antagonists (Figure 3a and b), suggesting that histamine upregulates periostin expression through H1R activation *in vitro*.

Next, we determined whether periostin was induced by histamine via H1R *in vivo*. Histamine release was triggered through mast cell degranulation using the compound 48/80 in WT and H1R-deficienct ($H1R^{-/-}$) mice. After treatment with compound 48/80 for three consecutive days, skin at the injected site was sampled. Periostin expression in WT and $H1R^{-/-}$ mouse skin was compared by western blotting analyses (Figure 3c). In WT mice, periostin expression markedly increased after compound 48/80 treatment, although no such increase was observed in $H1R^{-/-}$ mice (Figure 3c). These results suggest that H1R mediates histamine-induced periostin upregulation.

H1R activation upregulates periostin expression via the ERK1/2 pathway

Next, to investigate the signal transduction pathway involved after H1R activation by histamine in dermal fibroblasts, we used a commercial human phosphorylated kinase array kit to profile the phosphorylated kinases in normal human dermal fibroblasts (Figure 4a). Subsequently, phosphorylation of analogous kinases was confirmed in murine dermal fibroblasts by western blot analysis (Figure 4b). Compared with nontreated dermal fibroblasts, enhanced phosphorylation of extracellular signal-regulated kinase 1/2 (ERK1/2) and the downstream factor cAMP response element-binding protein (CREB) was observed after 10 minutes and 30 minutes of histamine stimulation (Figure 4a and b).

Furthermore, we found that histamine-induced phosphorylation of ERK1/2 and CREB was blocked not only with U0126 (a selective ERK1/2 kinase inhibitor) but also with an H1R antagonist (Figure 4c and d).

These observations demonstrated that histamine activates the ERK1/2 signal transduction pathway via H1R in dermal fibroblasts.

In addition, to verify the involvement of ERK1/2 activation in histamine-induced upregulation of periostin, western blotting analysis was performed (Figure 4c and d). Both U0126 and H1R antagonists decreased the expression of periostin, as well as suppressed the phosphorylation of CREB (Figure 4c and d). These results indicated that H1R-mediated signaling upregulated periostin expression via the ERK1/2 pathway.

H1R-mediated upregulation of periostin is essential for histamine-induced collagen production

To investigate the involvement of periostin in histamine-induced collagen production, primary dermal fibroblasts from WT and periostin-deficient ($PN^{-/-}$) mice were stimulated with histamine (100 μM) for 48 hours. The induction of collagen was abolished in $PN^{-/-}$ fibroblasts at both the mRNA (Figure 5a) and protein (Figure 5b and c) levels. Histamine-treated $PN^{-/-}$ fibroblasts did not exhibit increases in mRNA or protein expression of type I collagen (Col1; Figure 5a–c).

As described above, periostin was induced by histamine via the H1R pathway. To further clarify whether H1R was associated with histamine-induced collagen production, H1R antagonist was added to WT fibroblasts before histamine stimulation. After 48 hours of histamine stimulation, collagen production was evaluated as determined by quantitative real-time reverse transcriptase–PCR, Sircol Collagen Assay, and western blotting analyses (Figure 6). As expected, histamine-induced collagen synthesis was blocked by an H1R antagonist (Figure 6a–c). Furthermore, this inhibitory effect was rescued by the addition of recombinant mouse periostin (rmPeriostin; Figure 6a–c).

In addition, this mechanism was confirmed in cultured primary human dermal fibroblasts derived from healthy donor skin biopsies (Supplementary Figure S1 online).

Finally, we addressed the question of how strong the effect of histamine on tissue remodeling was in AD. Compared with normal skin and AD nonlesioned skin, increased expression of

periostin was observed in both acute AD lesioned skin and skin tissues with positive *Dermatophagoides farinae* (Derf1) scratch tests (Supplementary Figure S2 online). Our results suggest that histamine may contribute to the initiation of tissue remodeling during the acute phase of AD.

DISCUSSION

Here, we report that histamine increases the expression of periostin in dermal fibroblasts. Moreover, periostin increases *de novo* synthesis of Col1 via an ERK1/2-mediated pathway.

It is widely recognized that mast cells contribute to the healing of skin wounds (Hebda *et al.*, 1993; Artuc *et al.*, 1999; Trautmann *et al.*, 2000; Gailit *et al.*, 2001; Noli and Miolo, 2001). Impaired wound closure in mast cell–deficient mice indicates that mast cells have a crucial role in the wound repair process (Weller *et al.*, 2006). An increased number of mast cells in fibrotic tissues such as scleroderma, keloid, or healing wounds has been identified (Hawkins *et al.*, 1985; Atkins and Clark, 1987), although it is still unclear whether mast cells are fibrogenic. In many instances, chemical mediators, such as histamine, which is derived from degranulated mast cells or basophils, have been implicated as a cause of inflammation and tissue remodeling in AD (Davies and Greaves, 1980; Nishioka *et al.*, 1987; Wahlgren, 1999; Murota and Katayama, 2009). In support of these findings, H1R antagonist has been shown to inhibit the synthesis of Col1 by dermal fibroblasts (Murota *et al.*, 2008). Interestingly, histamine H1R antagonists but not H2R antagonists reduced wound closure in experimentally induced skin wounds in mice (Weller *et al.*, 2006). Therefore, histamine is believed to have an important role in the wound-healing process. Indeed, disruption of histamine in histidine decarboxylase knockout mice resulted in delayed cutaneous would healing, and this phenotype was rescued by exogenous histamine administration (Numata *et al.*, 2006). It remains unclear how histamine promotes wound healing. Some reports indicated that histamine induces fibroblast proliferation after a long period of coculturing (Russel *et al.*, 1977; Topol *et al.*, 1981). In our study, increased expression of Col1 mRNA was observed after 48 hours of co-incubation with histamine. Thus, histamine-mediated tissue remodeling may require the expression of periostin as a second messenger in order to elicit tissue remodeling.
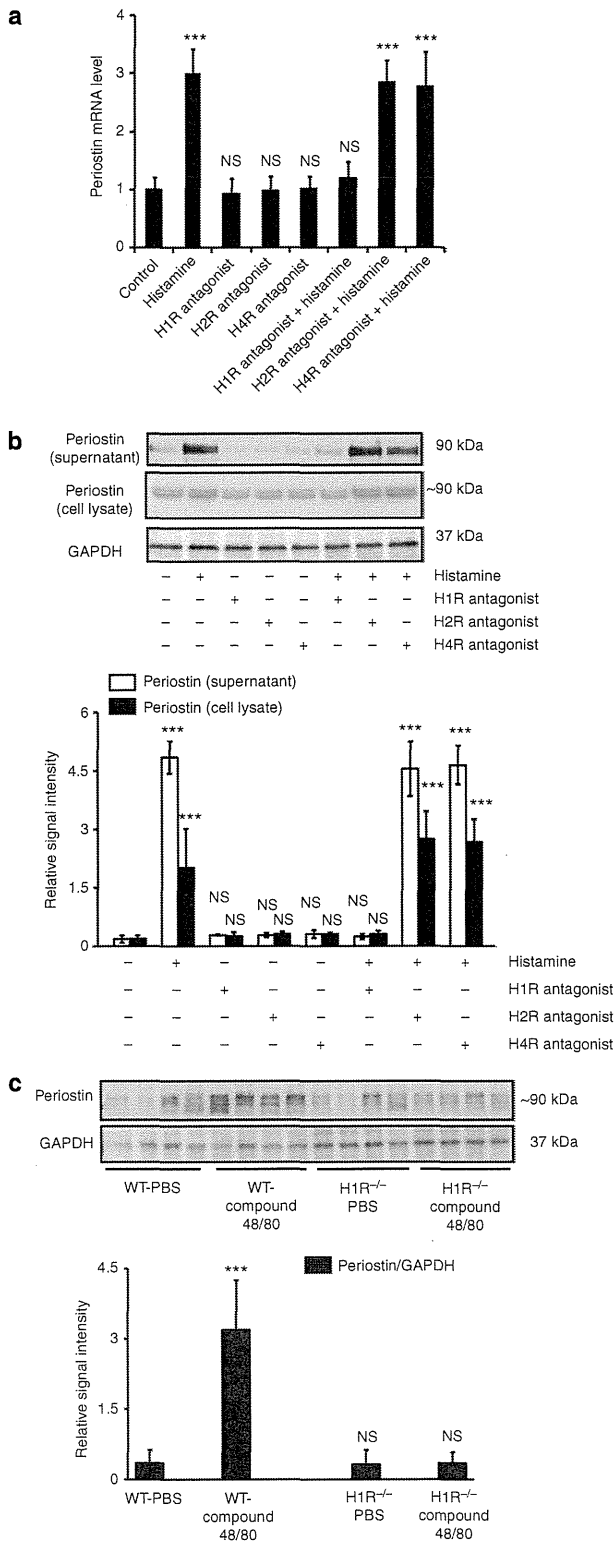

Figure 3. Histamine upregulates periostin expression via histamine receptor 1 (H1R) *in vitro* and *in vivo*. *In vitro*, wild-type (WT) fibroblasts were either treated with histamine antagonists (H1R, H2R, or H4R; 100 mM) or left untreated for 2 hours, and then cells were stimulated with histamine (100 μM) for an additional 2 hours (a) or 24 hours (b). Periostin expression was examined by quantitative real-time reverse transcriptase–PCR (qRT-PCR) (a) and western blotting analysis (b). *In vivo*, WT and *H1⁻ᐟ⁻* mice were treated with mast cell stimulator compound 48/80 for 3 days by subcutaneous injection, and periostin protein expression in the injected site skin was evaluated by western blotting analysis (*n* = 4 mice per group); representative blots and quantitative analysis of signal density on blots from four mice of each group are shown (using glyceraldehyde 3-phosphate dehydrogenase (GAPDH) as an internal control). (c) Values in **a** and **b** are shown as mean ± SD for three independent experiments. Values in **c** are shown as mean ± SD for blot signals from four mice. ***$P<0.001$; NS, no significance, compared with control (0 μM histamine in **a** and **b**; WT-phosphate-buffered saline in **c** by one-way analysis of variance (ANOVA) followed by Dunnett's test.
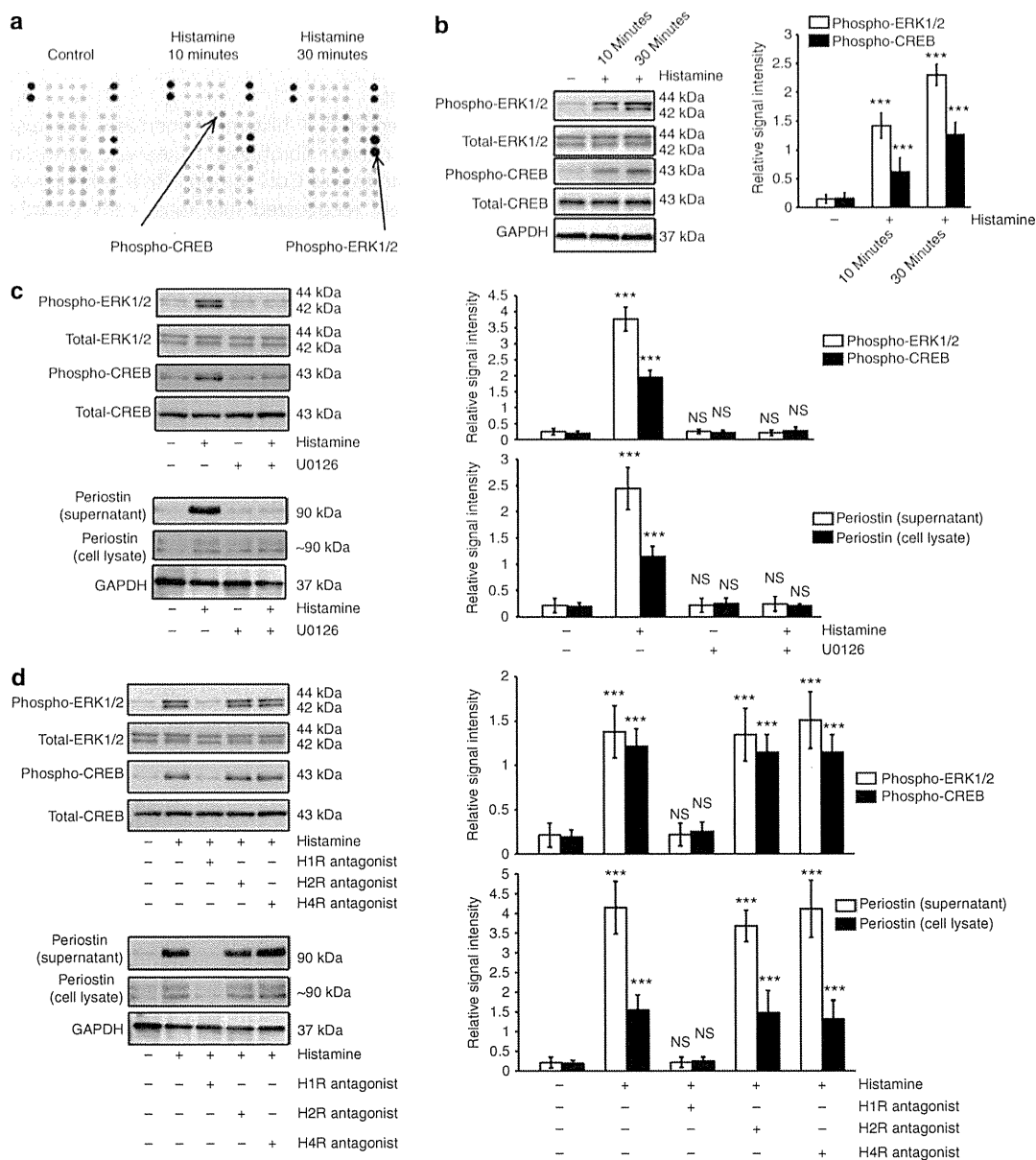
Figure 4. Histamine receptor 1 (H1R) activation upregulates periostin expression via the extracellular signal-regulated kinase 1/2 (ERK1/2) pathway. (a) The phosphorylation state was detected by R&D Systems Proteome Profiler Phospho-Kinase Array in normal human dermal fibroblasts, which were either untreated or treated with histamine for 10 minutes or 30 minutes. The activated kinases are indicated by arrows. (b) Phosphorylated ERK1/2 and phosphorylated cAMP response element-binding protein (CREB) were evaluated by western blotting analyses in murine wild-type (WT) fibroblasts following histamine stimulation for 10 minutes and 30 minutes. (c) WT fibroblasts with or without ERK1/2 inhibitor (U0126, 20 μm) preincubation were stimulated with histamine (30 minutes, upper panel; 24 hours, lower panel). Phosphorylated ERK1/2, phosphorylated CREB, and periostin protein expression was examined by western blotting analyses. (d) WT fibroblasts cultured in the presence or absence of preincubation with histamine receptor antagonists (H1R, H2R, or H4R; 100 mm) were stimulated with histamine (30 minutes, upper panel; 24 hours, lower panel). Phosphorylated ERK1/2, phosphorylated CREB, and periostin protein expression was examined by western blotting analyses. Three independent experiments were performed, and representative blots and quantitative analysis of signal density on blots from three independent experiments are shown (using glyceraldehyde 3-phosphate dehydrogenase (GAPDH) as an internal control). ***$P<0.001$; NS, no significance, compared with control (0 μm histamine) by one-way analysis of variance (ANOVA) followed by Dunnett's test.

Periostin, a recently characterized matricellular protein, has been reported to have crucial roles in tooth and periodontium development (Horiuchi *et al.*, 1999), cancer proliferation and invasion (Siriwardena *et al.*, 2006; Baril *et al.*, 2007; Kudo *et al.*, 2012), cardiac healing after acute myocardial infarction

(Shimazaki *et al.*, 2008), idiopathic interstitial pneumonia (Okamoto *et al.*, 2011), and bone marrow fibrosis (Oku *et al.*, 2008). Furthermore, periostin is highly expressed in connective tissue and at the remodeling tissue site after injury or inflammation. This protein is secreted from fibroblasts via
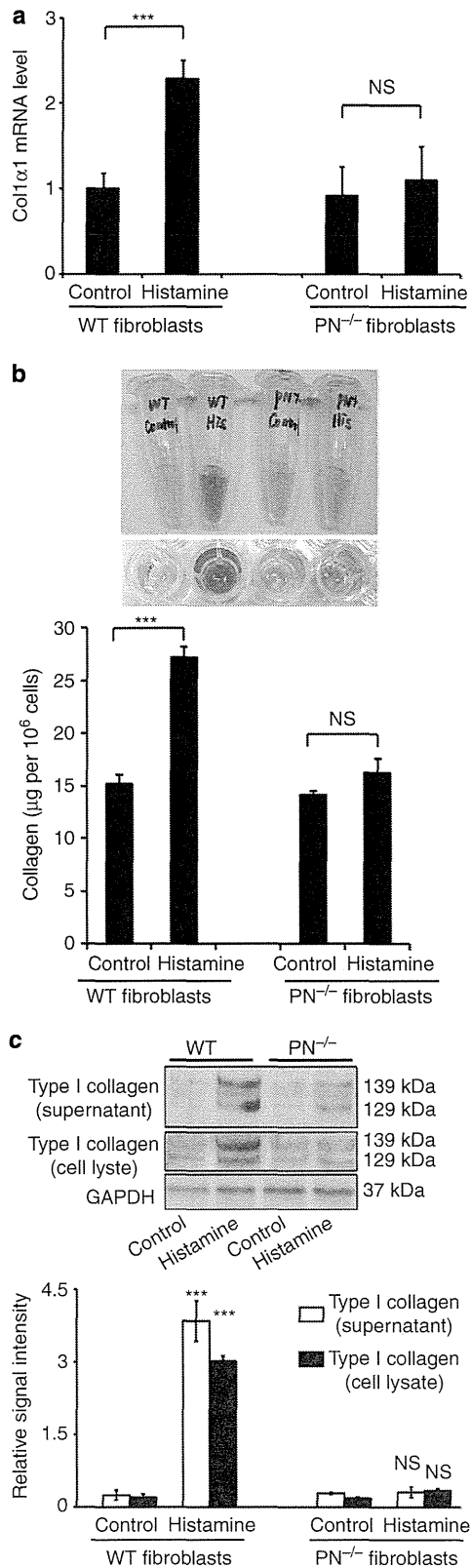
transforming growth factor beta stimulation (Horiuchi *et al.*, 1999). Periostin was shown to accelerate cardiac healing after acute myocardial infarction (Dorn, 2007; Oka *et al.*, 2007; Shimazaki *et al.*, 2008) and during full-thickness cutaneous wound repair (Nishiyama *et al.*, 2011; Elliott *et al.*, 2012; Ontsuka *et al.*, 2012) by modulating fibroblast differentiation.

Periostin has also been reported to be induced by other factors, including bone morphogenetic proteins, vascular endothelial growth factor, connective tissue growth factor, vitamin K, IL-3, IL-4, IL-6, and IL-13 (Asano *et al.*, 2005; Takayama *et al.*, 2006; Iekushi *et al.*, 2007; Blanchard *et al.*, 2008; Coutu *et al.*, 2008; Banerjee *et al.*, 2009; Norris *et al.*, 2009). Recently, the increased expression of periostin was confirmed in various allergic diseases such as bronchial asthma (Takayama *et al.*, 2006), AD (Masuoka *et al.*, 2012), and eosinophilic chronic rhinosinusitis (Hur *et al.*, 2012). As an IL-4- and IL-13-inducible protein, periostin is associated with tissue remodeling in bronchial asthma (Takayama *et al.*, 2006), allergic eosinophilic esophagitis (Blanchard *et al.*, 2008), AD (Masuoka *et al.*, 2012), and allergic rhinitis (Hur *et al.*, 2012). In the present study, histamine was found to directly induce periostin expression, whereas the expression levels of transforming growth factor beta, IL-4, and IL-13 were not altered by histamine stimulation (data not shown). Thus, we postulate that periostin is involved in the initiation of tissue remodeling in chronic allergic diseases.

AD is known to develop tissue remodeling, which is characterized by epidermal thickening, hyperkeratosis and fibrosis of the papillary dermis, increased fibroblast proliferation, and collagen accumulation, and these features are caused by nonspecific stimuli, constant scratching, and rubbing (Lee *et al.*, 2009). Tissue remodeling and repair are thought to be the underlying causes of chronic allergic inflammation, such as in asthmatic diseases and AD (Leung, 1995). Recently, increased expressions of periostin and the inducers of periostin (IL-4, IL-13, and transforming growth factor beta) were identified in a screening of AD-associated genes in genome-wide association studies and quantitative mRNA expression analysis in lesion tissues (Hoffjan and Epplen, 2005; Wood *et al.*, 2009a, 2009b). Furthermore, in the present study, elevated expression of periostin was found in lesional skin of patients with AD. These results suggest that periostin may be involved in AD and in asthma.

Figure 5. **Periostin is essential in histamine-induced collagen production in vitro.** Primary dermal fibroblasts from wild type (WT) and periostin-deficienct ($PN^{-/-}$) mice were stimulated with histamine (100 μM) or phosphate-buffered saline (PBS) (control) for 48 hours. The collagen type-I alpha 1 (Col1α1) mRNA level was examined by quantitative real-time reverse transcriptase–PCR (qRT-PCR) (a), and collagen protein expression was evaluated by Sircol assay (b) and western blotting analysis; representative blots and quantitative analysis of signal density on blots from three independent experiments are shown (using glyceraldehyde 3-phosphate dehydrogenase (GAPDH) as an internal control) (c). Values are shown as mean ± SD for three independent experiments. ***P<0.001; NS, no significance, compared with paired control (WT fibroblasts control or $PN^{-/-}$-fibroblasts control) by Student's *t*-test.

In WT and $PN^{-/-}$ mice, a mite extract–induced AD model was established and analyzed. In contrast to WT mice, $PN^{-/-}$ mice showed amelioration of epidermal hyperplasia and

inflammatory cell infiltration (Masuoka *et al.*, 2012). Moreover, periostin directly induces production of thymic stromal lymphoprotein in keratinocytes (Masuoka *et al.*, 2012). Thus, periostin was suggested to have a critical role in the amplification and chronicity of allergic skin inflammation.

The results of the present study demonstrate the role of periostin in histamine-mediated collagen production. We found that H1R-mediated phosphorylation of ERK1/2 had a crucial role in histamine-induced collagen production. These observations may open a new window of therapeutic opportunity against airway remodeling in asthma or dermal remodeling in AD, as histamine H1R anatagonists are expected to ameliorate tissue remodeling.

As refractory chronic allergic symptoms are known to impair the quality of life, work productivity, and overall activity (Meltzer *et al.*, 1999; Thompson *et al.*, 2000; Kawashima *et al.*, 2002; Baiardini *et al.*, 2003; Spector *et al.*, 2007), we believe that these studies will provide a basis for exploring the fibrotic components of allergic diseases in skin and other tissues.

MATERIALS AND METHODS

Mice

WT mice (C57BL/6 strain) were purchased from CLEA Japan (Osaka, Japan). Periostin gene knockout ($PN^{-/-}$) mice (C57BL/6 strain) were generated as previously described.(Shimazaki and Kudo, 2008) Histamine receptor 1 gene knockout ($H1R^{-/-}$) mice (C57BL/6 strain) were purchased from Oriental Bio Service (Kyoto, Japan). Mice were maintained in our pathogen-free animal facility. Animal care and experimentation were performed in accordance with the institutional guidelines of the National Institute of Biomedical Innovation, Osaka, Japan and Osaka University, Osaka, Japan. Six-week-old male mice were used in all experiments. All experiments used four mice per group.

Compound 48/80 treatment

Compound 48/80 (Sigma, St Louis, MO) was dissolved in phosphate-buffered saline at a concentration of 1 $mg\,ml^{-1}$ and sterilized by filtration. With the use of a 27-gauge needle, 100 µl of compound 48/80 or phosphate-buffered saline was subcutaneously injected into the back side of mice each day for 3 days. One day after the final injection, the skin at the injected site was removed and solubilized at 4 °C in lysis buffer (0.5% sodium deoxycholate, 1% Nonidet P40,
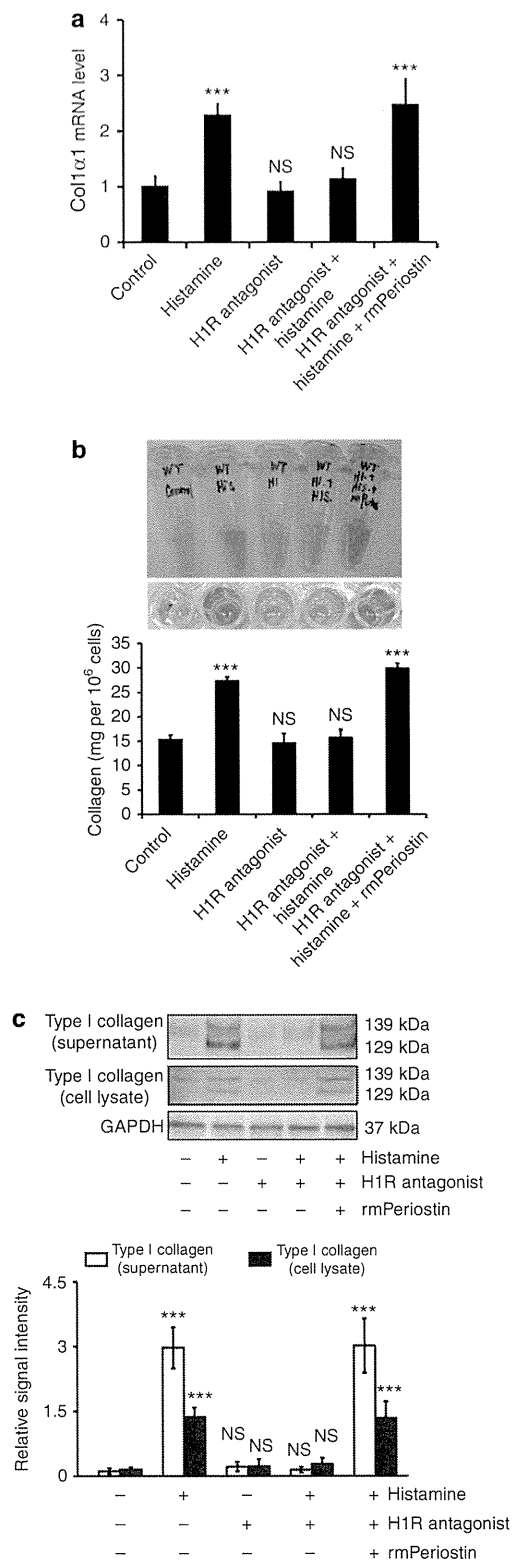
Figure 6. **Histamine receptor 1 (H1R)-mediated upregulation of periostin is essential in histamine-induced collagen production.** Wild-type (WT) fibroblasts cultured with or without H1R antagonist preincubations were stimulated with histamine (100 µM) alone or in the presence of recombinant mouse periostin (rmPeriostin, 100 ng/ml^{-1}). The collagen type-I alpha 1 (Col1α1) mRNA level was examined by quantitative real-time reverse transcriptase–PCR (qRT-PCR) (a), and collagen protein expression was evaluated by Sircol assay (b) and western blotting analysis; representative blots and quantitative analysis of signal density on blots from three independent experiments are shown (using glyceraldehyde 3-phosphate dehydrogenase (GAPDH) as an internal control) (c). Values are shown as mean ± SD for three independent experiments. ***$P<0.001$; NS, no significance compared with control (0 µM histamine) according to one-way analysis of variance (ANOVA) followed by Dunnett's test.